Nanoanalysis of Defects in Perovskites

Manfred Rühle

MPI für Metallforschung, Heisenbergstr. 3,
70569 Stuttgart, Germany

Microscopy of Materials:
Domain Structure in Ferroelectric $BaTiO_3$

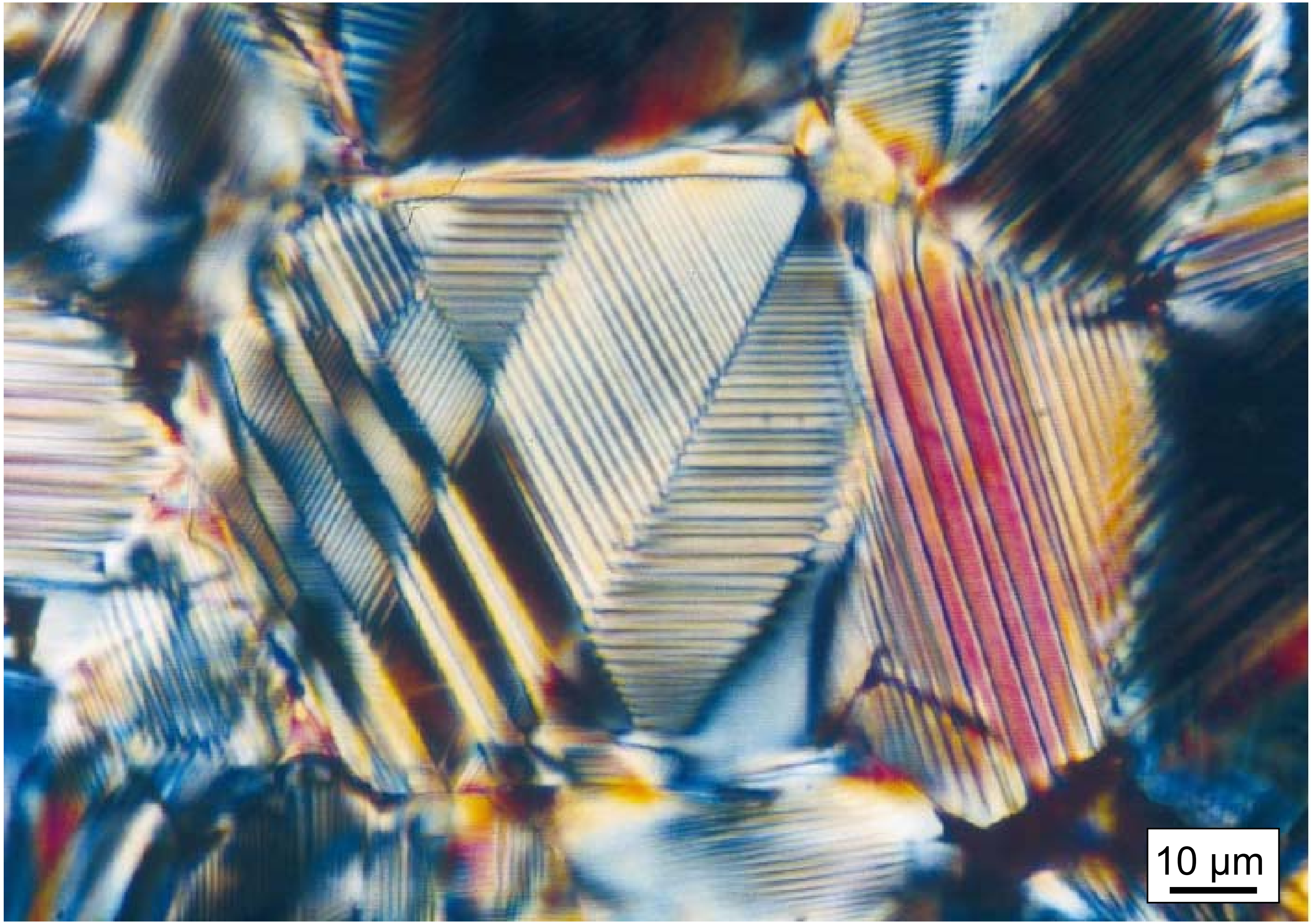

Materials Science

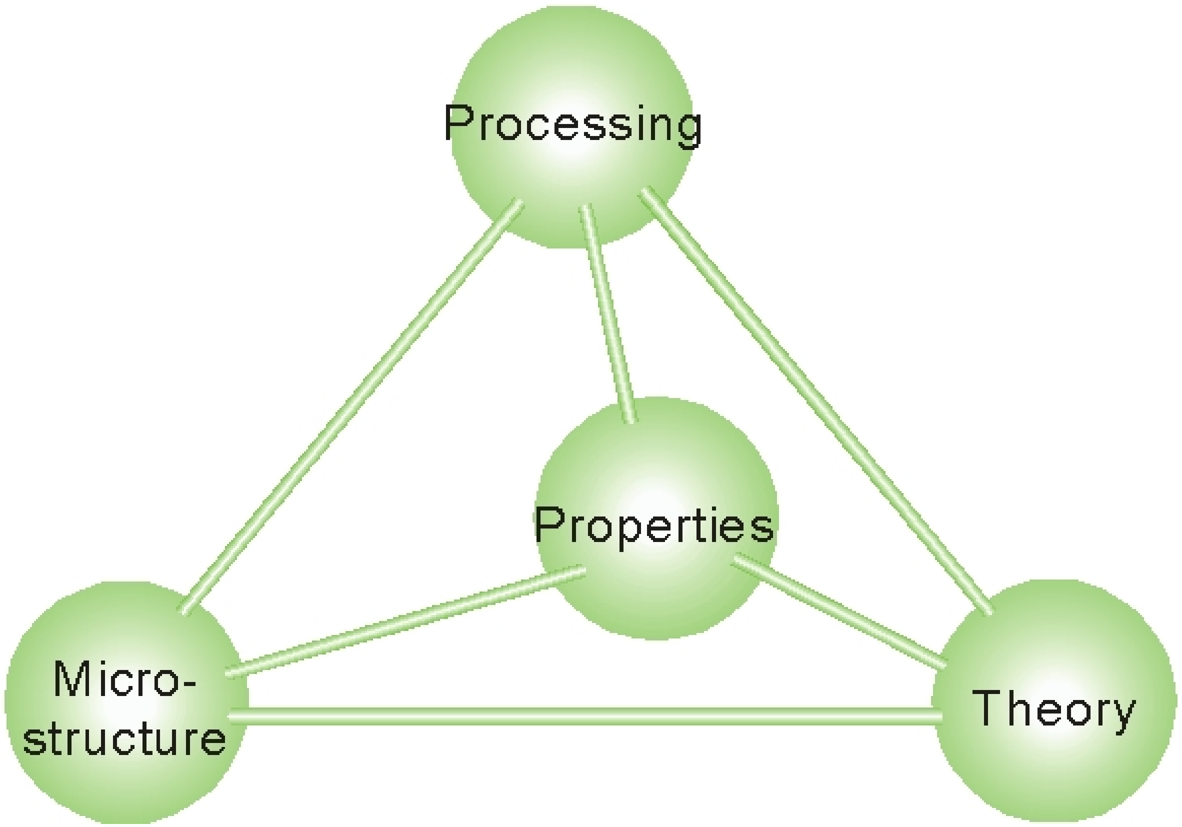

holds also for Nanomaterials!

Processing:
Sintering
Thin film growth
Solid State Diffusion Bonding

Properties:
mechanical properties
electrical and magnetic properties
electronic properties

Microstructure:
characterisation on different length scales
to atomic level
Nanoanalysis

Theory:
modelling on different length scales
- ab initio
- atomistic with phenomenological potentials
- FEM technique
- continuum modeling

Microstructure and Dimensions of Defects

Microstructure: (Mikrostruktur, Gefüge)

Microstructure describes all deviations from perfect material in thermodynamic equilibrium:

- point defects (vacancies, interstitials)	0-dimensional defects
- line defects (dislocations)	1-dimensional defects
- planar defects (stacking faults, domain boundaries, internal interfaces)	2-dimensional defects
- large particles	3-dimensional defects

Microstructure at all Length Scales

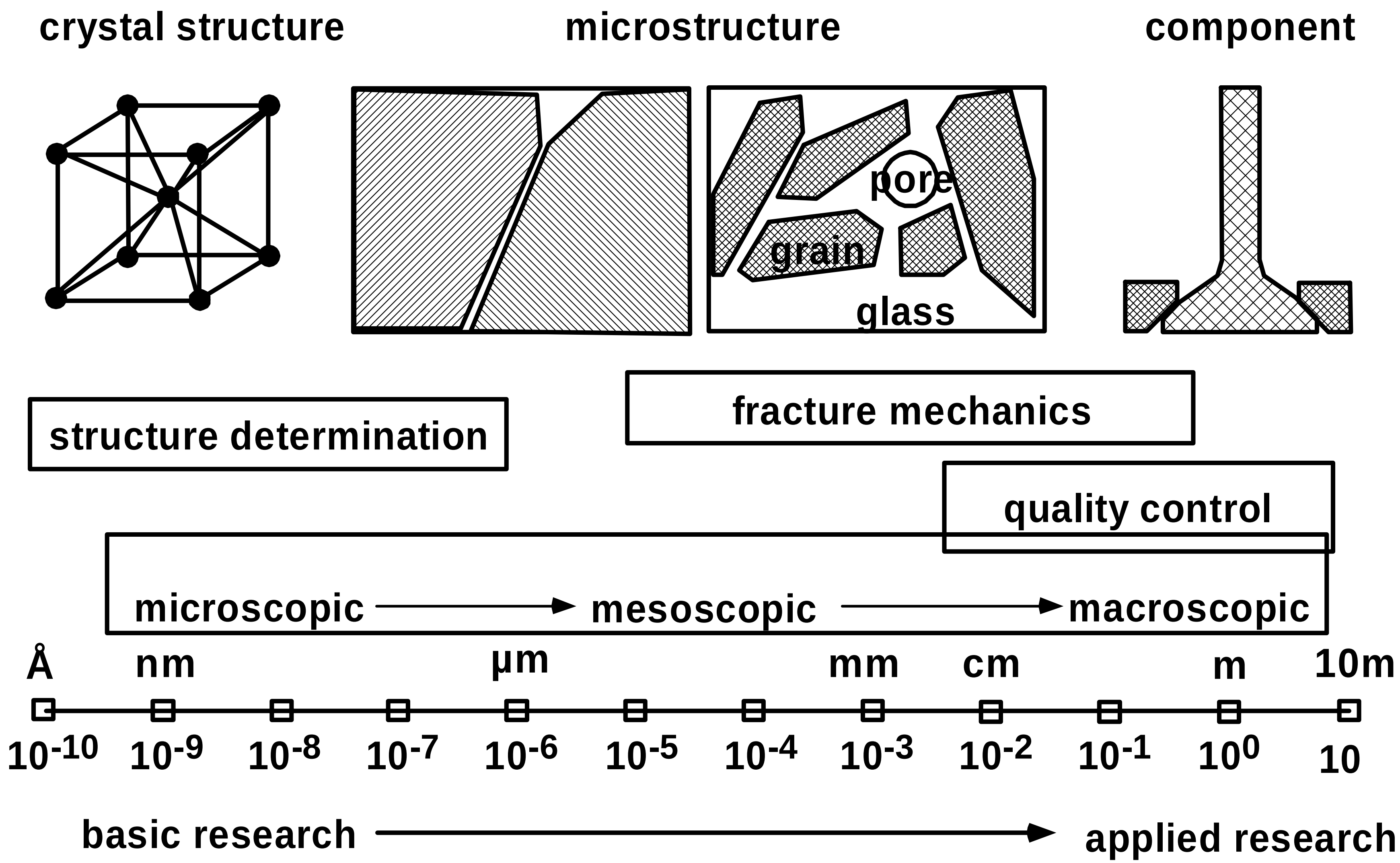

Microstructural Features that Influence Properties

feature

grains
- size distribution
- shape, aspect ratio
- distribution of differently shaped grains

second phases
- nature
- frequence
- distribution
- size, location

texture
- grain shape
- grain orientation
- frequencey and distribution (clustering?)

mm → µm

grain boundaries (GB) and phase boundaries (GB)
- shape
- GB-plane
- facetting

"special" boundaries
- cyrstallography
- type, structure

µm → nm

GB chemistry
- segregation
- type of segregant
- distribution
- amorphous film
- structure of segregated GB phase

nm → Å

length scale

Social History of Materials Scientists (late 20th century)

Classicalists	Solid State Ph or C	Heat + Beat
Constructionalists	Atom by Atom	Spray + P(r)ay
Neo-Constructionalists	Soft Chemistry	Mix + Fix
Post-Constructionalists	Self-Assembly	Match + Catch
Re-Constructionalists	Biomimetics	Take + Fake

Outline

Introduction
Microscopy on all length scales
Perovskites: Strontium titanate (STO)
    Defects: Dislocations and grain boundaries
Interfaces between Pd/STO
Summary and Conclusions

Acknowledgements

Microstructure:	O. Kienzle, F. Ernst, S. Hutt, K. v. Benthem, B. Rahmati, W. Sigle, Z. Zhang
Theory:	M. Finnis (Belfast), C. Elsässer, R. Janisch
Mech. Properties:	S. Taeri, D. Brunner
Specimen Preparation:	U. Salzberger, A. Strecker, M. Sycha

Financial Support:
German Science Foundation (DFG) trough Grad. Kolleg
State of Baden Württemberg
EC-NSF Projects: NANOAM and INCEMS

Microscopy of Materials:
Domain Structure in Ferroelectric $BaTiO_3$

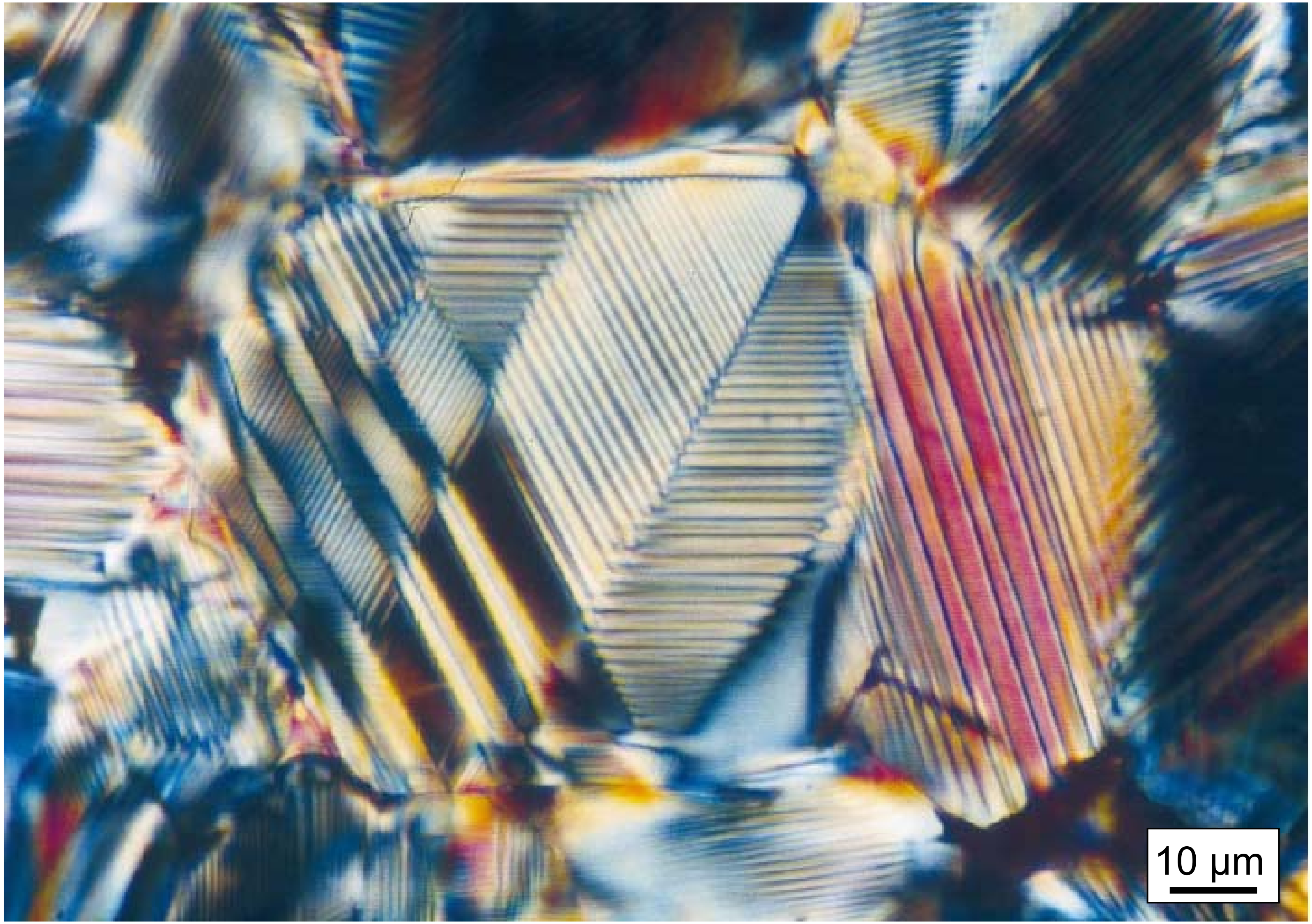

Robert Hooke (1665)
Principle of a Microscope

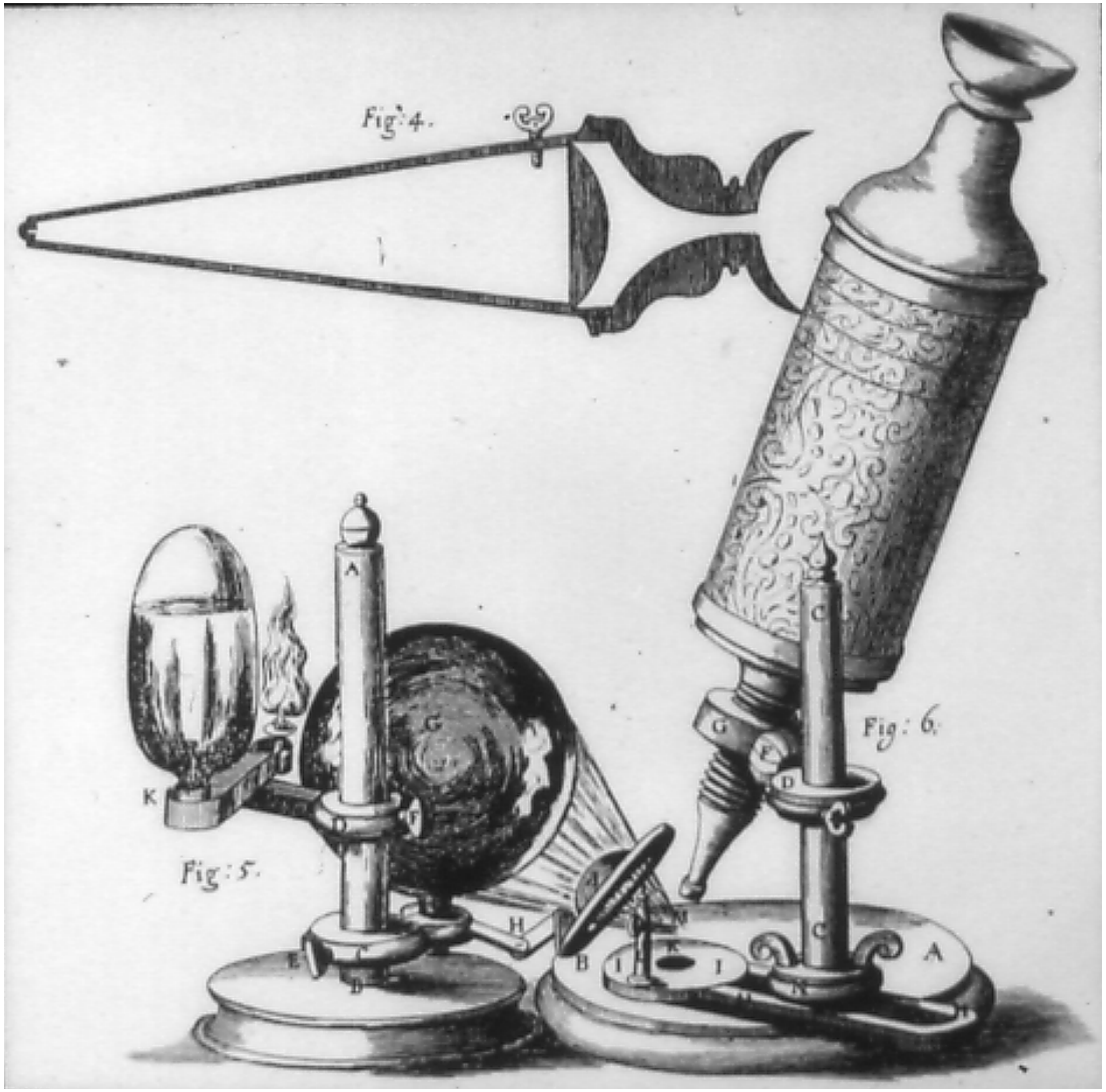

Observations in a Microscope can be Unpleasant

Abb. 1. »Thames Water«, Stich von William Heath um 1828.

Limits of Resolution of an Imaging System (Wave Optics)

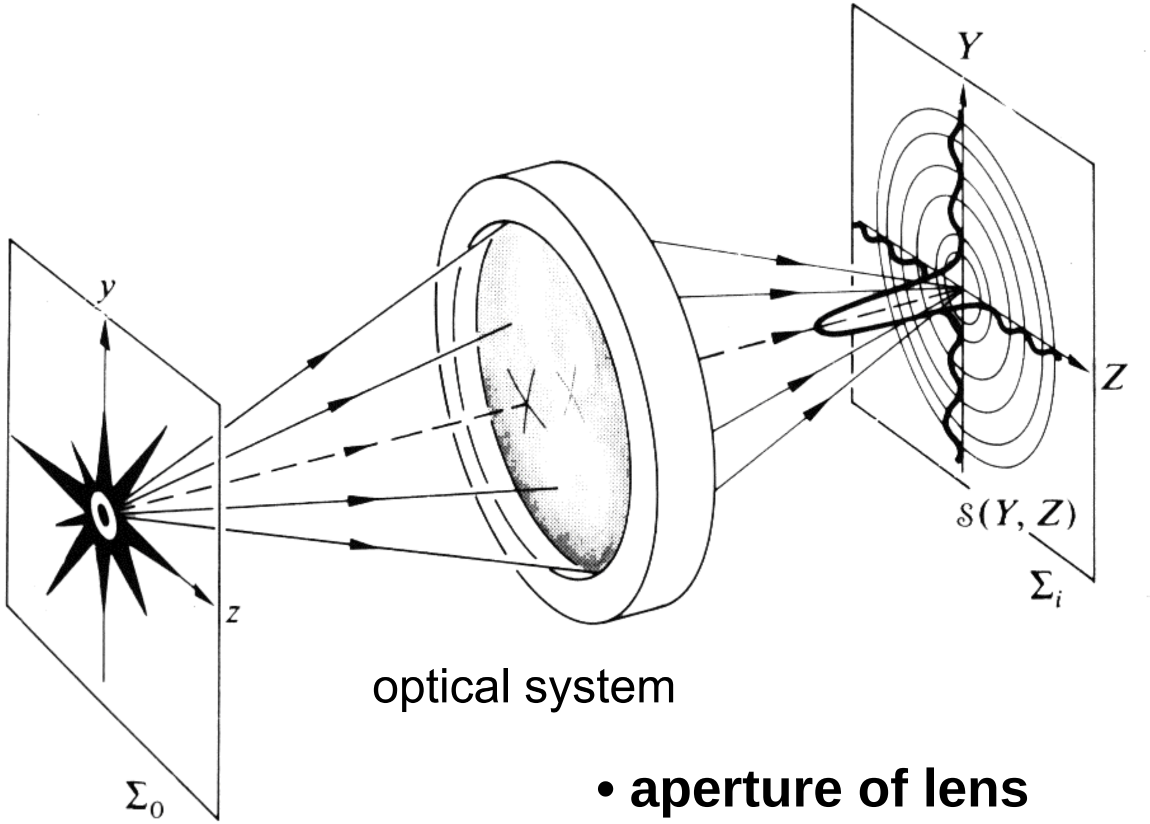

optical system

- **aperture of lens**
- **resolution:** $\mathbf{d_{min} = 0.5 \frac{\lambda}{n \sin\theta}}$

[minimal distance of 2 points (inΣ_0) which can be resolved in image plan Σ_i]

Essential Components of Microscope

- Source of light, radiation
- lenses for probe formation (condensor lenses)

  specimen

  image forming lenses

  objective lenses

  projector lenses
- detection system

lenses: convex

concave

Important Lens Aberrations

Spherical Aberration

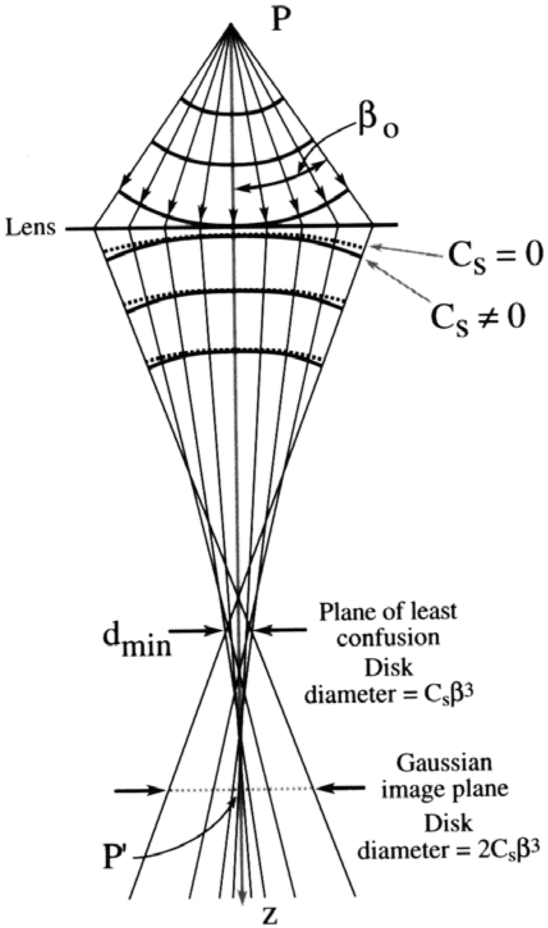

C_s spherical aberration coefficient

Chromatic Aberration

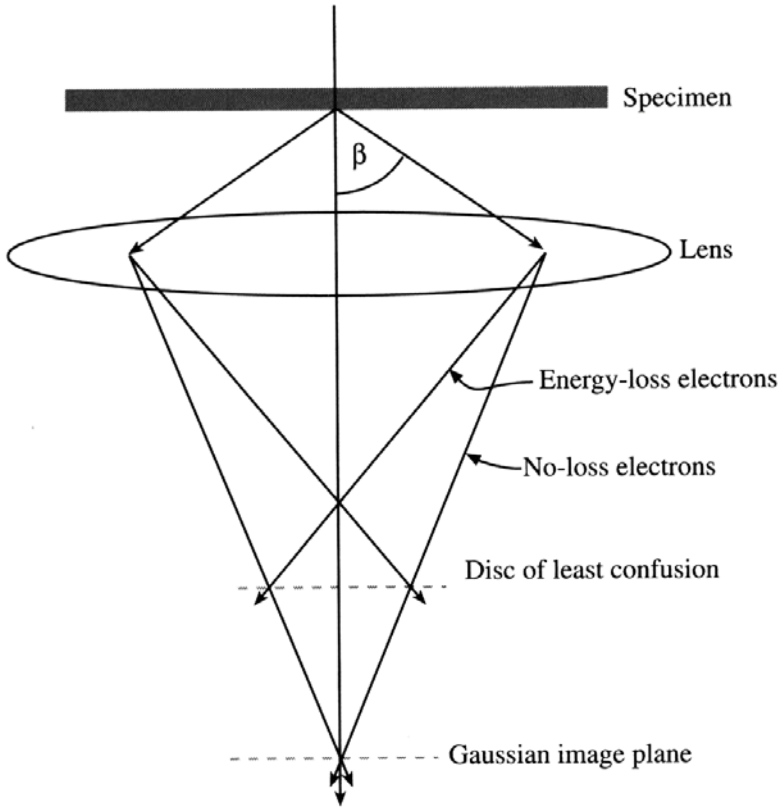

C_c chromatical aberration coefficient

correction of aberration: system (combination) of lenses (convex and concave)

Fundamentals for TEM

electron	m, e
acc. electrons	v, λ
lenses for electrons	inhomogeneous magn. fields (spherical aberrations)
interactions of electrons with solids	elastic scattering inelastic scattering
detection systems	film, electron plate, CCD camera
theoretical description	Bethe, Cowley, Hirsch, Howie

Length Scales in Microstructural Studies

Structural aspect

HRTEM	SEM	Optical Microscope
< 0.1 nm	10 nm	1 µm

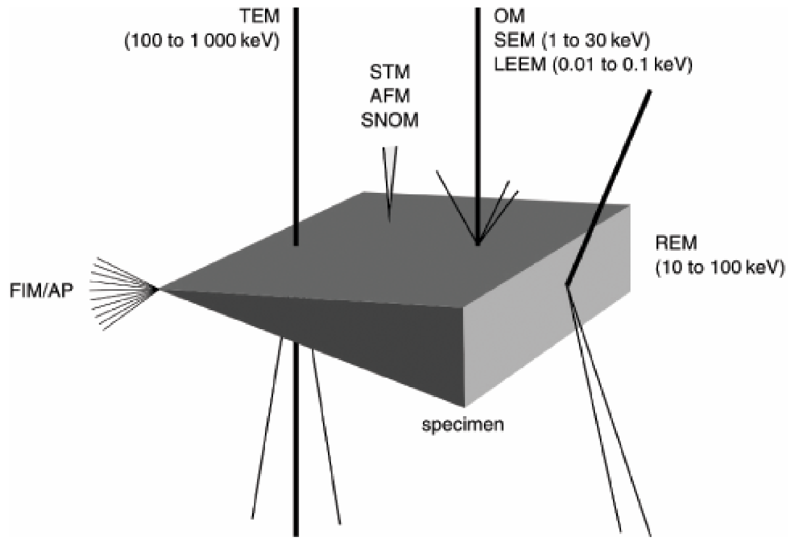

Chemical aspect

individual atoms	10 - 100 atoms	overall composition
3 - DAP	Microprobe	wet
AEM	AEM	chemical
		analytical

Wavelength, Wavevector and Resolution in Electron Microscopy

U [kV]	λ [pm]	exp. resolution (θ = 10°) [pm]	real resolution [pm]
100	3.7	~21 (0.2Å)	300 (3.0Å)
200	2.51	~14 (0.14Å)	250 (2.5Å)
400	1.644	~9	170 (1.7Å)
1250	0.736	~4	90 (0.9Å)

lenses: rotationally symmetrical non-homogeneous magnetic fields

problem: spherical aberration, chromatic aberration

Words — Picture — Movie

One Picture is more than 1000 words

A Movie is more than 1000 pictures

Assumption:

Picture is interpretable

Movie is interpretable

TEM Techniques

Transmission Electron Microscopy

Conventional TEM

BF/DF/SAD

- Morphology
- Phase Distribution
- Defect Analysis
- *in situ*-Experiments
  - heating
  - cooling
  - deformation

Spectroscopy and CBED

(high spatial resolution)

- EDS
  - compositions
  - gradients
- EELS
  (EXELFS, ELNES)
  - compositions
  - gradients
  - electronic states

Lattice Imaging

HREM

- Structure of materials
  - oxides
  - HT superconductors
- Structure of defects
  - interfaces
  - dislocations

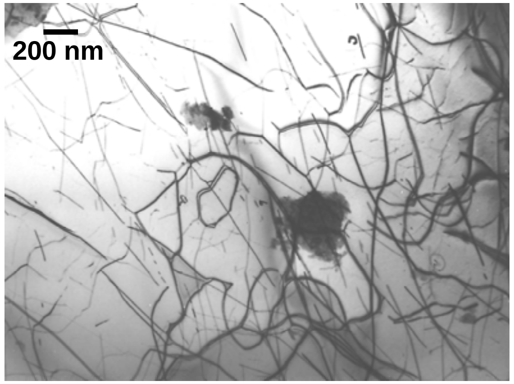

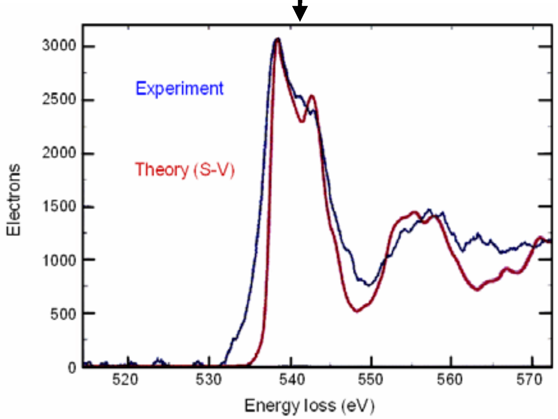

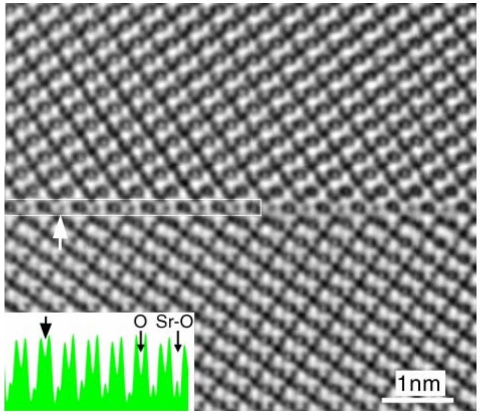

The Need for 3D Analysis: Tomography

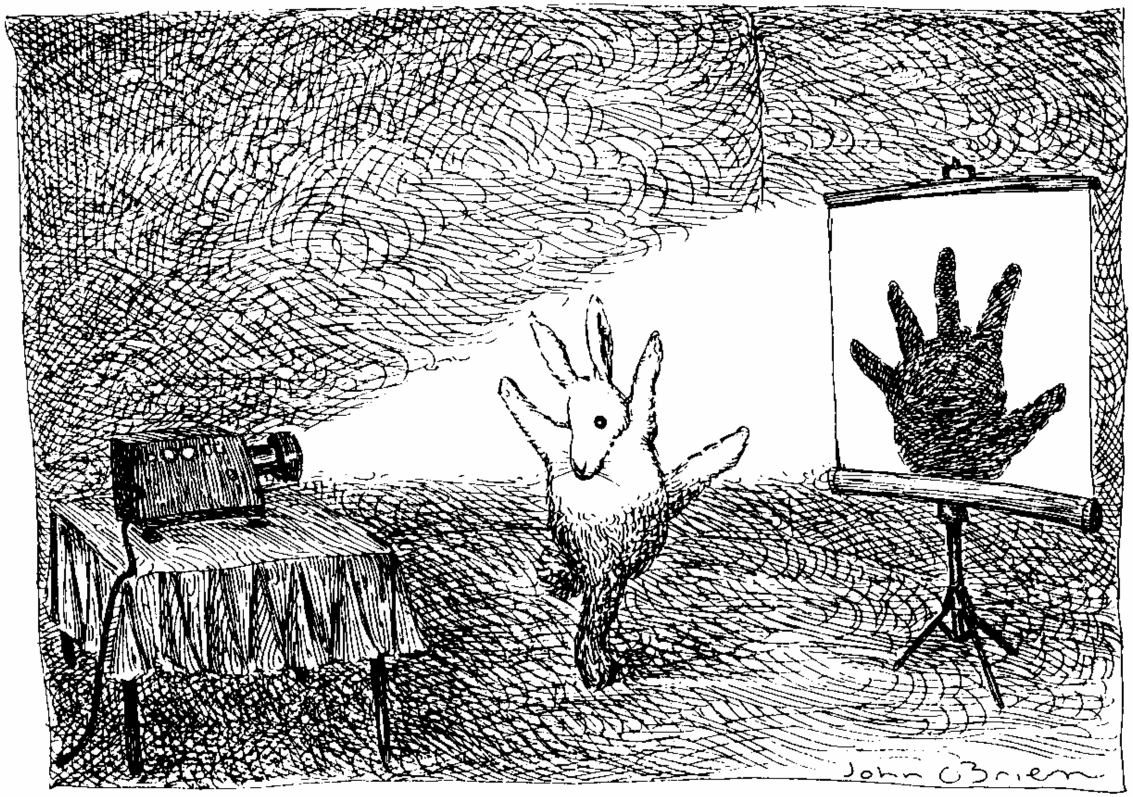

Fig. 5.1. A single projection image is plainly insufficient to infer the structure of an object. Drawing by John O'Brien; © 1991 The New Yorker Magazine.

By looking only in projection we can be fooled !

The Instrument

STUTTGART ARM

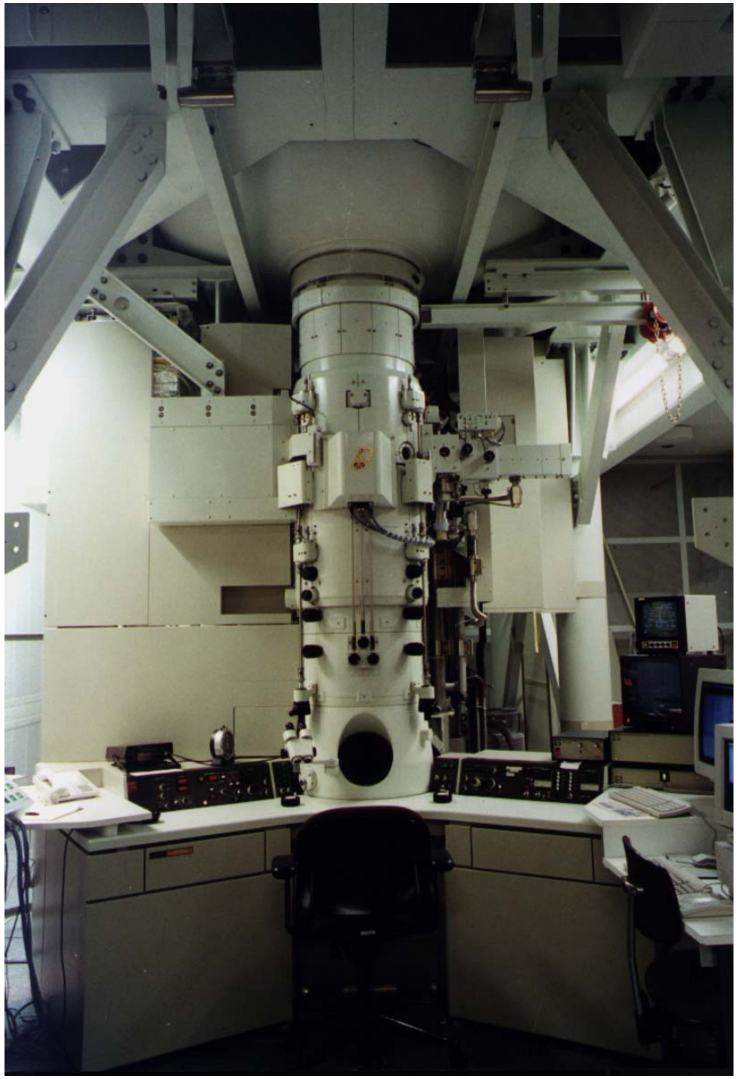

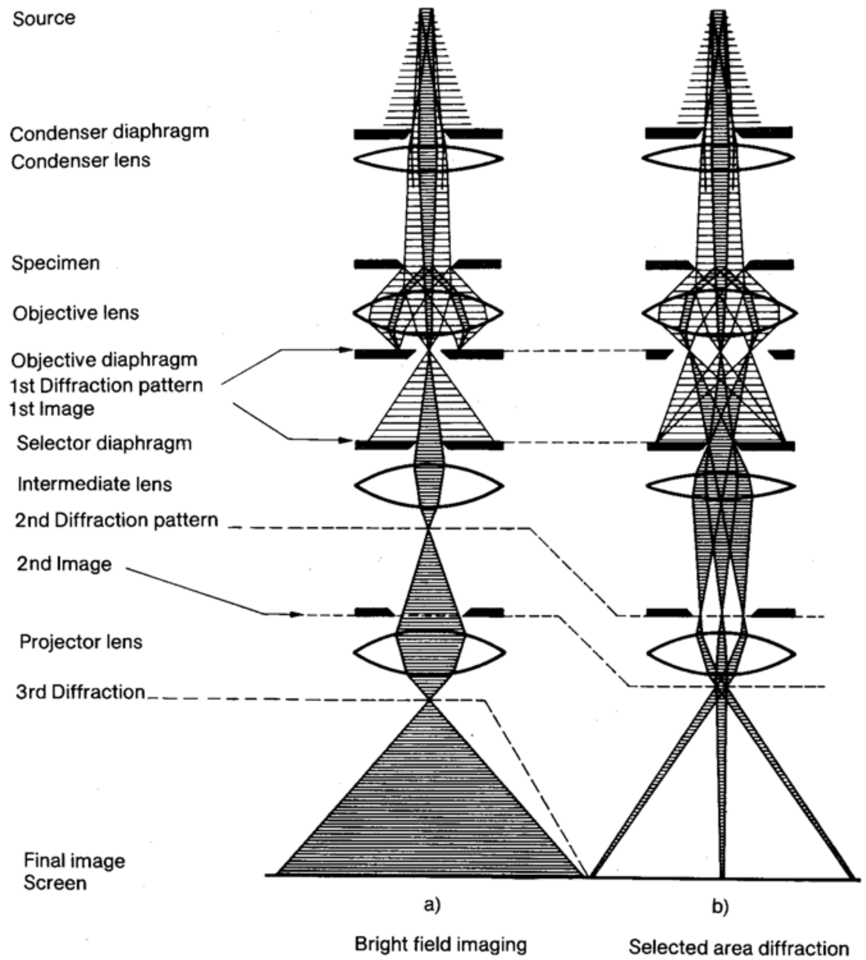

Advanced TEM Techniques

coherent parallel illumination

dedicated STEM

TEM - specimen
t: ≤ 250 nm CTEM
≤ 20 nm HRTEM
AEM

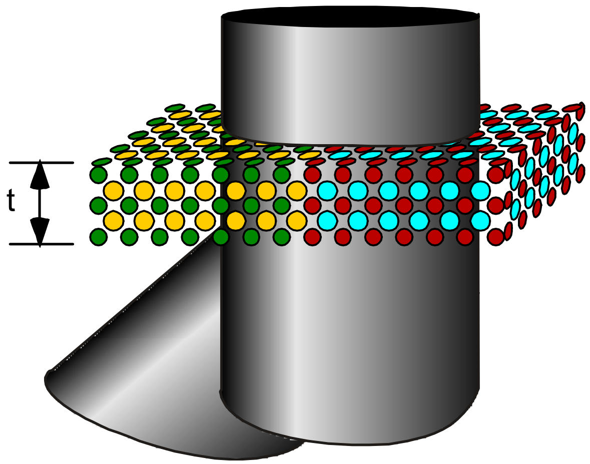

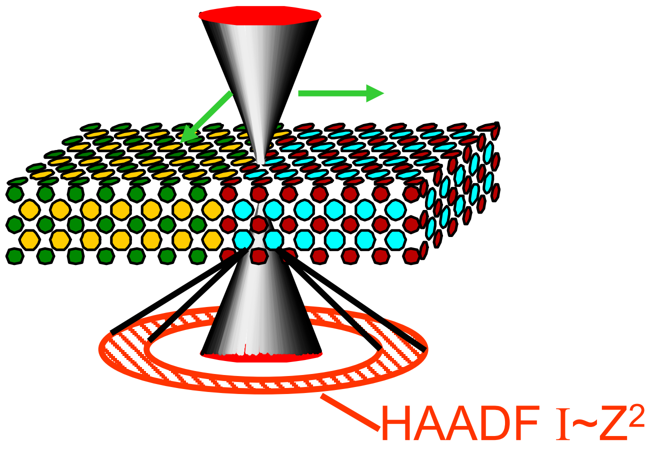

	beam diameter
parallel illumination: CTEM, HRTEM (coherent)	50 ... 100 nm
convergent illumination: HAADF, AEM	≤ 0.1 nm

C_s corrected illumination system

CTEM: Conventional TEM, HRTEM: High-Resolution TEM, AEM: Analytical Electron Microscopy

HAADF: High-angle annular dark field

Advanced TEM Techniques

Crystalline Materials

Incoming electron beam
parallel (or nearly parallel)
to the lattice planes

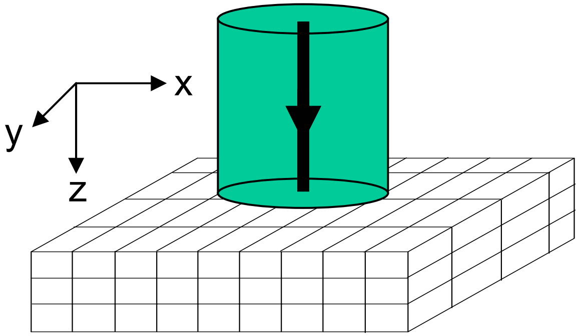

Object periodic in (x,y,z)

generates:
- Diffraction patterns (**DP**)
- Images (**I**)

Interpretation of **DP** and **I** is possible

Amorphous Materials

Incoming electron beam

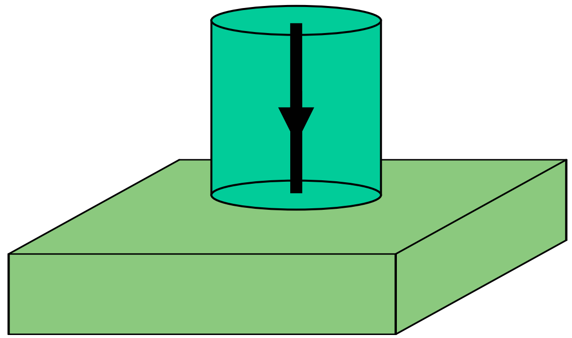

Object non-periodic

generates:
DP and **I**
Interpretation is difficult or impossible

CNT

Incoming electron beam

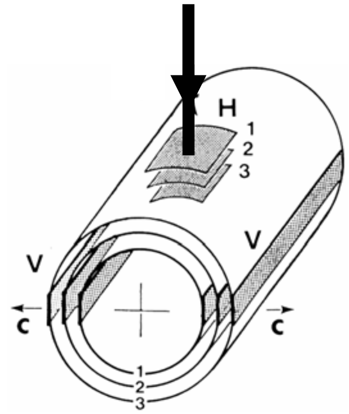

Object periodic || CNT axis

generates:
DP and **I**
Interpretation (to atomic level) is difficult

Only projection of a 3D object is investigated!

High-Resolution Electron Microscopy of Defects in a Thin Specimen

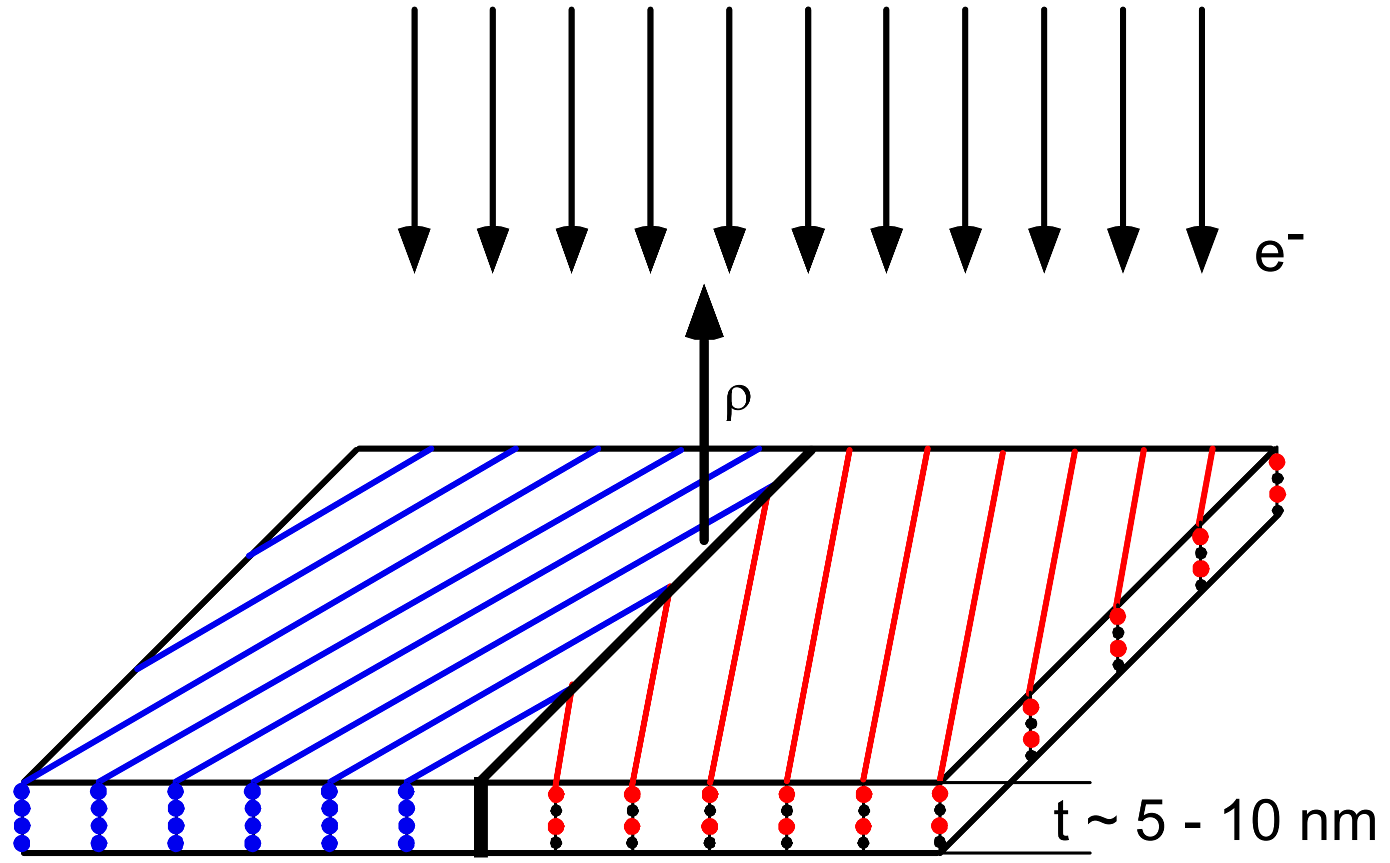

tomography (at least 2 projections for 3D information)

geometrical constraints limit applicability of HRTEM

Quantitative High-Resolution Transmission Electron Microscopy

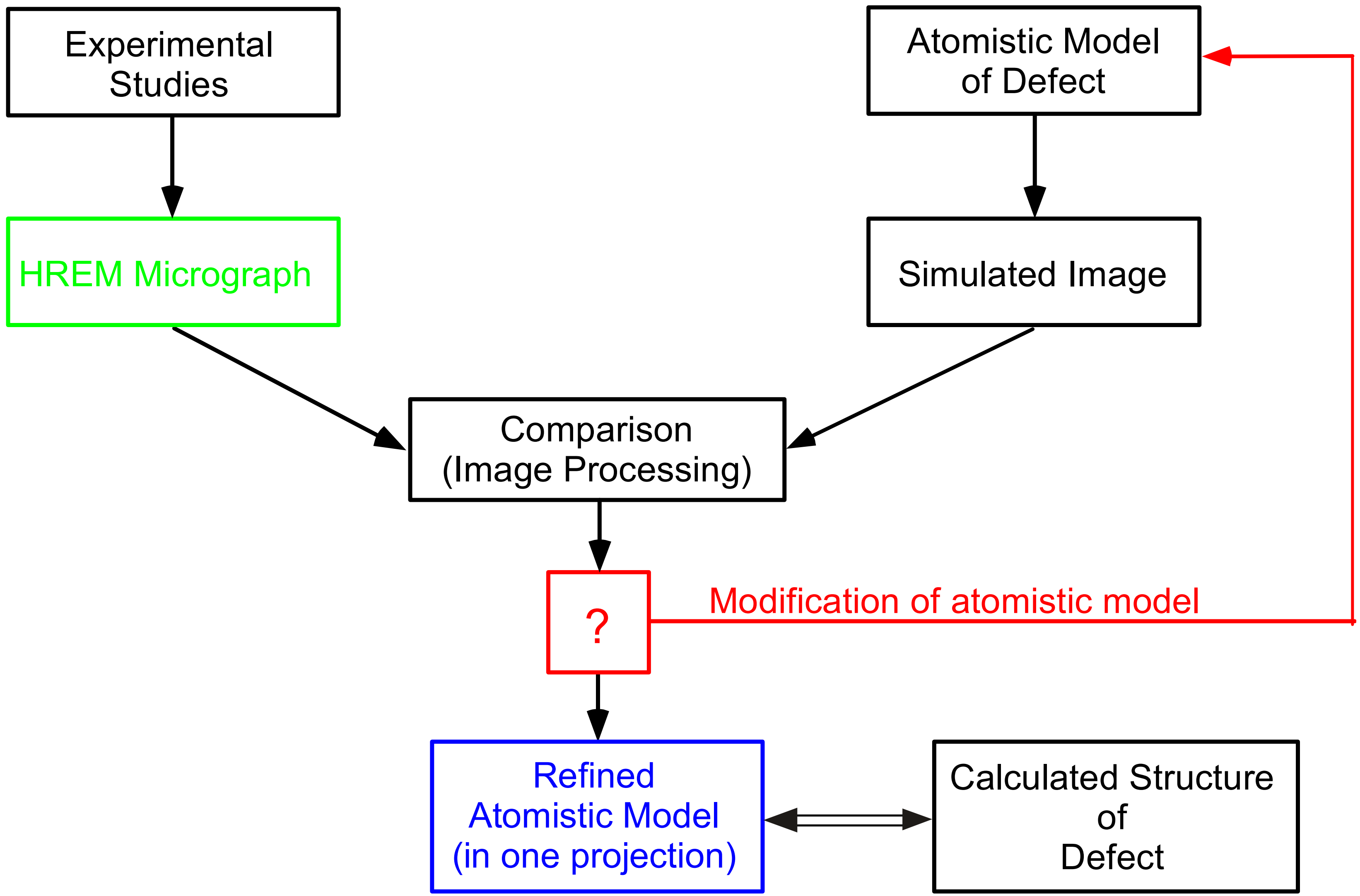

Elastic and Inelastic Scattering Process

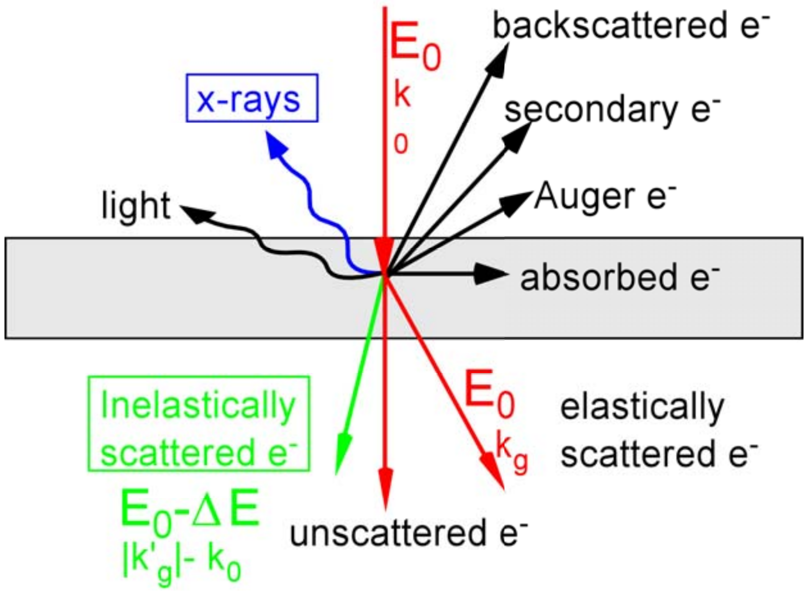

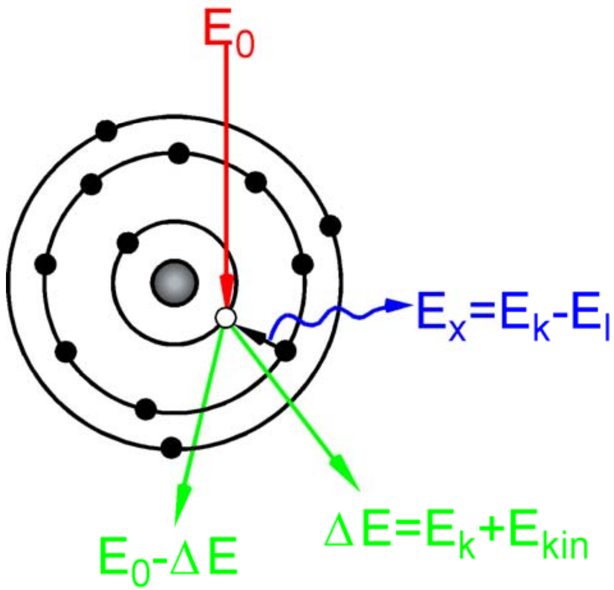

EDS
Energy Dispersive Spectroscopy

EELS
Electron Energy Loss Spectroscopy

ELNES
(Electron-Energy-Loss Near Edge Structure)

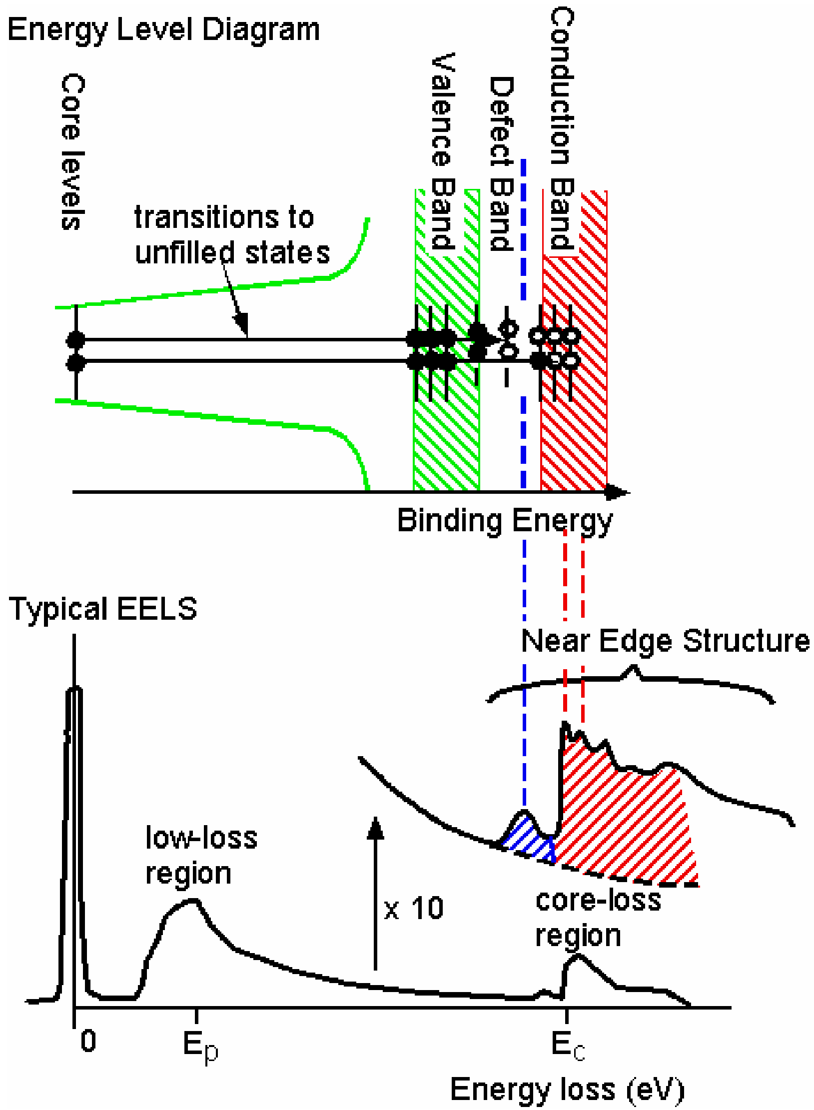

optical properties

Quantitative Evaluation:

- comparison to calculated ELNES spectra (DFT calculations)
- "finger printing"
  (comparison of experimental image to ELNES structure of known materials)
- Interface component of ELNES
  - Local spectrum with fine probe (smallest diameter)
  - spatial difference technique

Result:

Information on Bonding across Interfaces

ELNES

Information on the Surroundings of an Atom (in a crystal)

Electron Energy-Loss Near Edge Structure

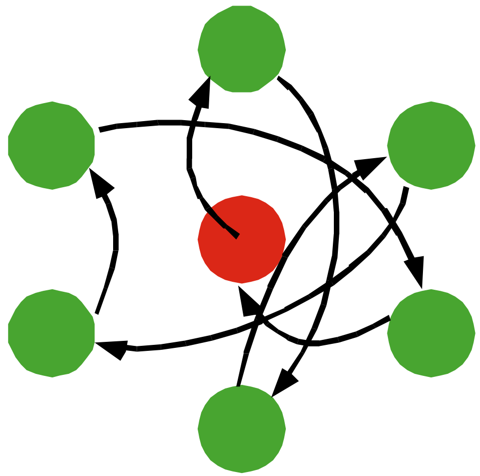

reflects mainly the **short range order** of the material

calculation from theory in **real space** via multiple elastic scattering (intershell and intrashell) of the excited electron within a cluster of atoms

contains information about environment of an atom:
coordination, bond length and chemical state

Very important for Nanoanalysis!

Models of Grain Boundaries (CSL)

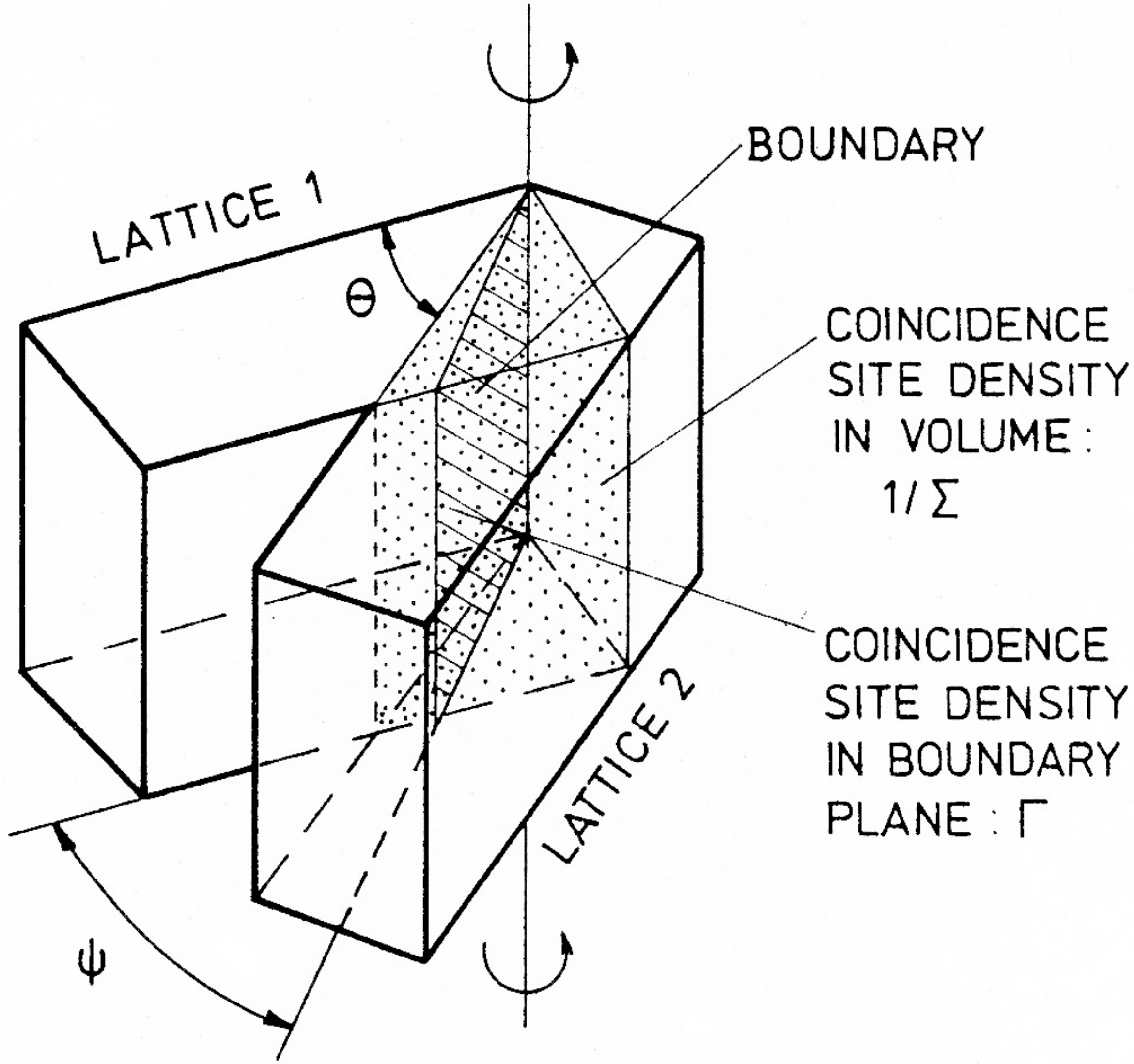

Coincidence Site Lattice (CSL) Model

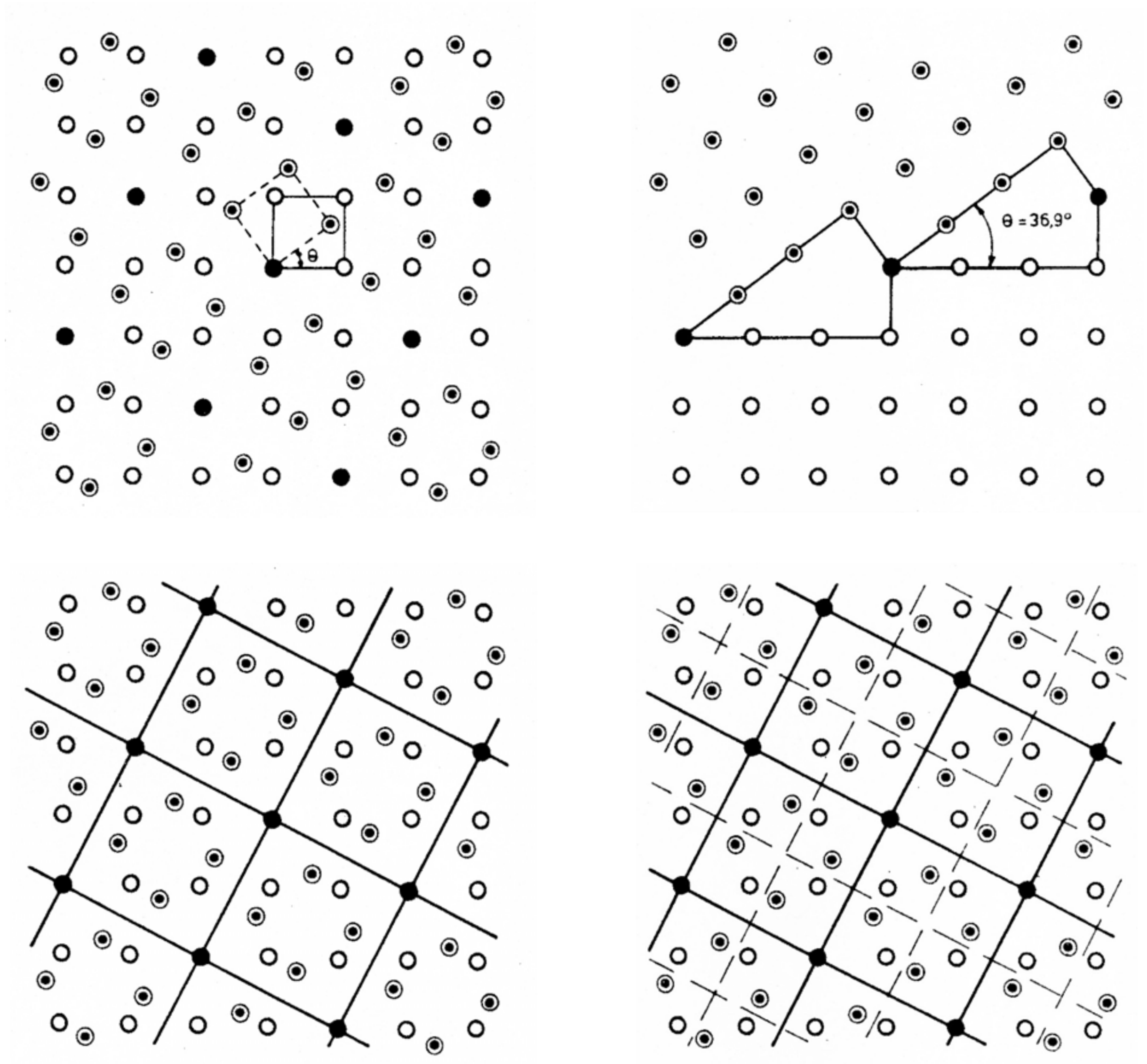

First principle Calculations for Σ 5 Boundary in STO

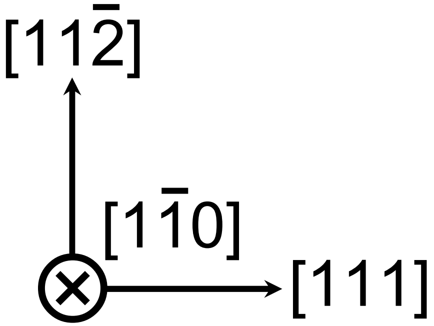

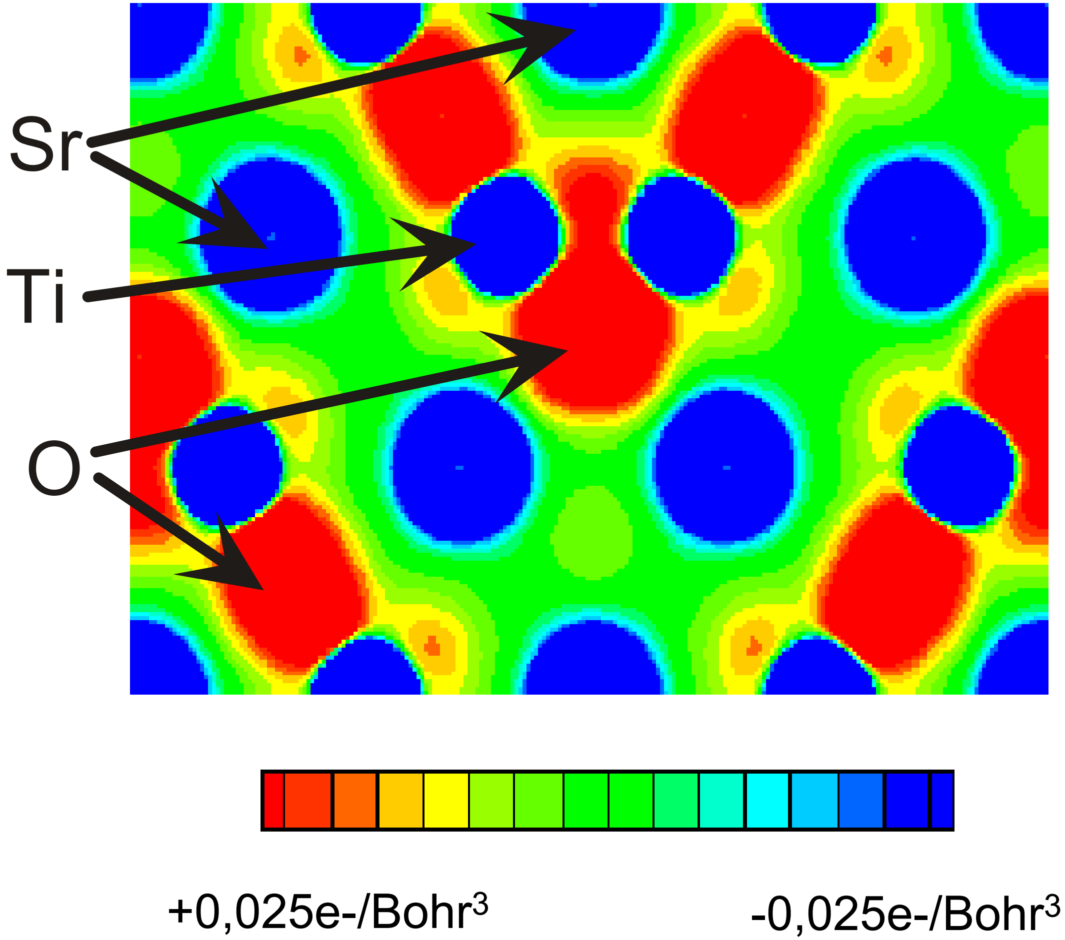

C. Elsässer, S. Hutt

STO: Some Fundamentals

perovskite structure

$Pm\bar{3}m$; a= 0.3905 nm

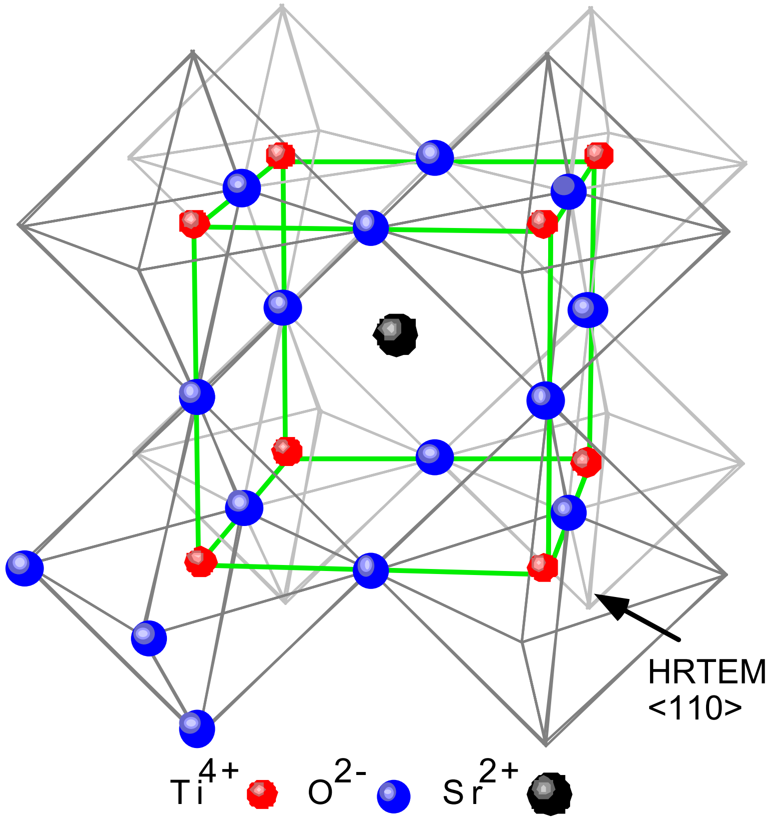

Electron Density distribution
by quantitative CBEM
(J. Mayer et al)

Usually doping of $SrTiO_3$
with Fe or Nb

(100) Surface:
etching with NH_4F-HF
results in TiO_2-terminated surface

STO some fundamentals

Perovskite: $A\ B\ O_3$

● Sr^{2+}

• Ti^{4+}

○ O^{2-}

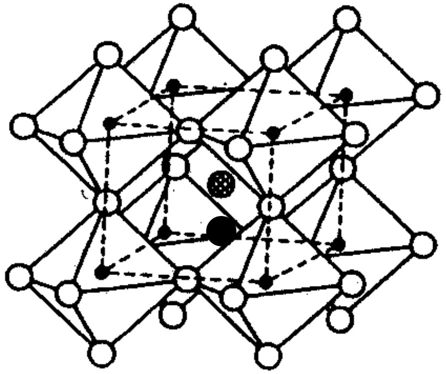

Charged Defects:

- ionic: $V_{Sr}^{''}$ $\quad$ ~~$V_{Ti}^{''''}$~~ $\quad$ $V_O^{\bullet\bullet}$
- electronic: e' , $h^{\bullet}$

Neg. Charged Defect: (´)

Pos. Charged Defect: (•)

Donor Doping: Nb^{5+} ⟶ Ti^{4+} replaces ➡ $Nb_{Ti}^{\bullet}$

e' OR $V_{Sr}^{''}$

electronic ionic

Compensation mechanism

Sr^{2+} (r = 0.132 nm)
Ti^{4+} (r = 0.075 nm)
Nb^{5+} (r = 0.068 nm)

B. Rahmati (2004)

STO: Some Fundamentals

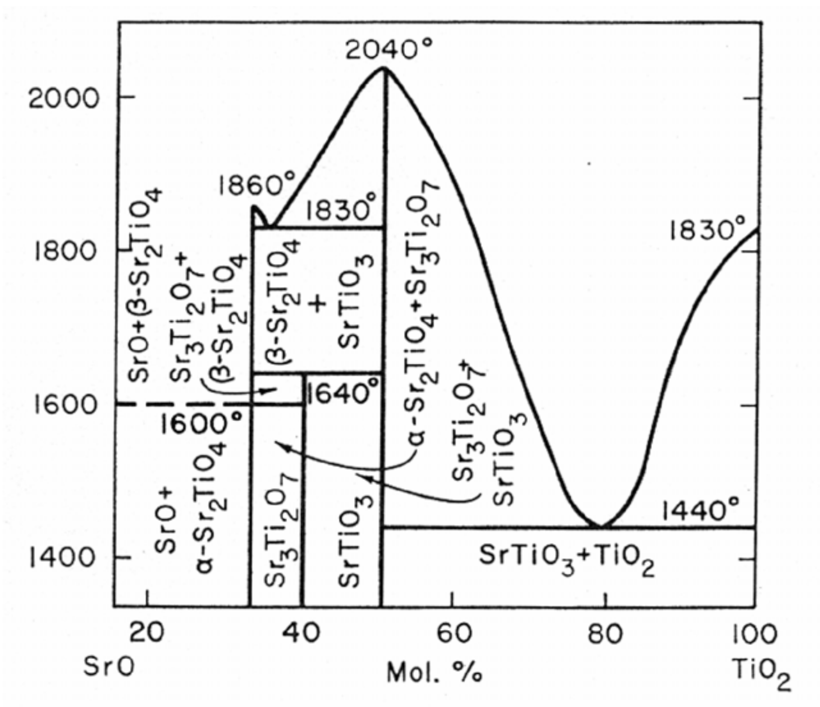

Pseudo-binary phase diagramme
$SrO – TiO_2$

space charge region

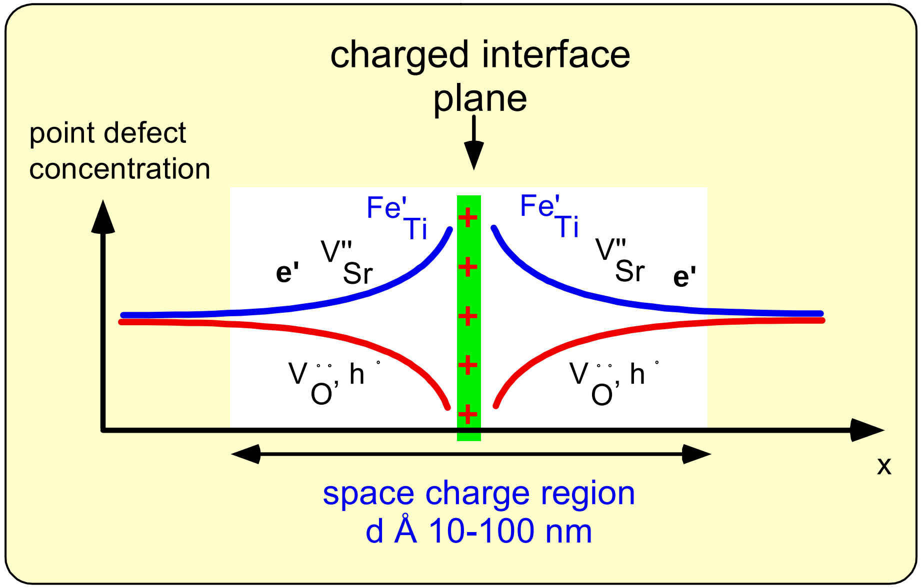

Model for space charge zones

Compensation mechanism depends strongly on processing conditions (T, P(O_2), [D]) !!!

Sintering under low P(O_2) ~ 10^{-10}-10^{-20} atm:

Reduction: $$O_O^{\times} \rightarrow V_O^{\bullet\bullet} + 2e' + \frac{1}{2}O_2$$

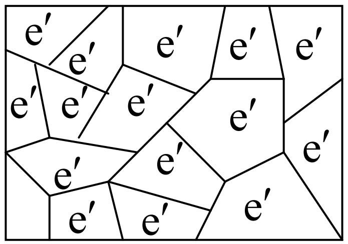

$$Nb_{Ti}^{\bullet} \leftrightarrow e'$$

Semiconducting

Post-sintering under O_2: P(O**2**) = 1 atm.

Reoxidation: $$\frac{1}{2}O_2 + V_O^{\bullet\bullet} + 2e' \rightarrow O_O^{\times}$$

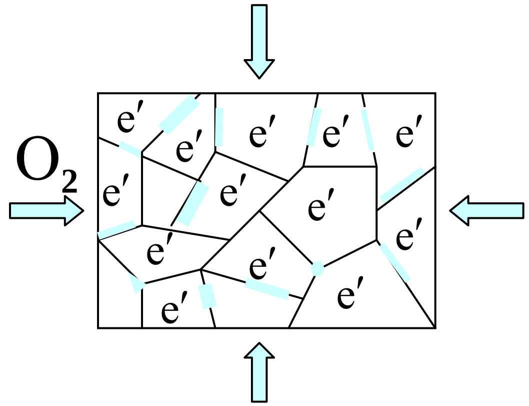

$$O_O^{\times} + Sr_{Sr}^{\times} \rightarrow SrO + V_O^{\bullet\bullet} + V_{Sr}''$$

$$Nb_{Ti}^{\bullet} \leftrightarrow V_{Sr}''$$

Insulating GB region

$$Nb_{Ti}^{\bullet} \leftrightarrow e'$$

Semiconducting grains

B. Rahmati (2004)

Studies at GBs in Bicrystals of STO

Fabrication of well defined bicrystals with symmetrical g.b.

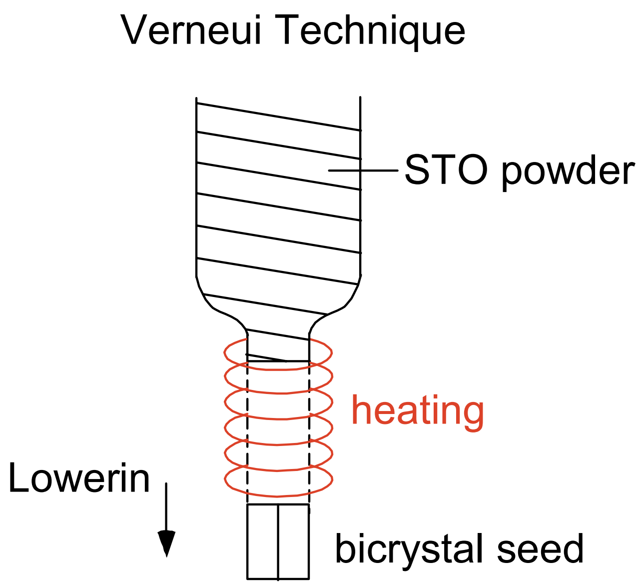

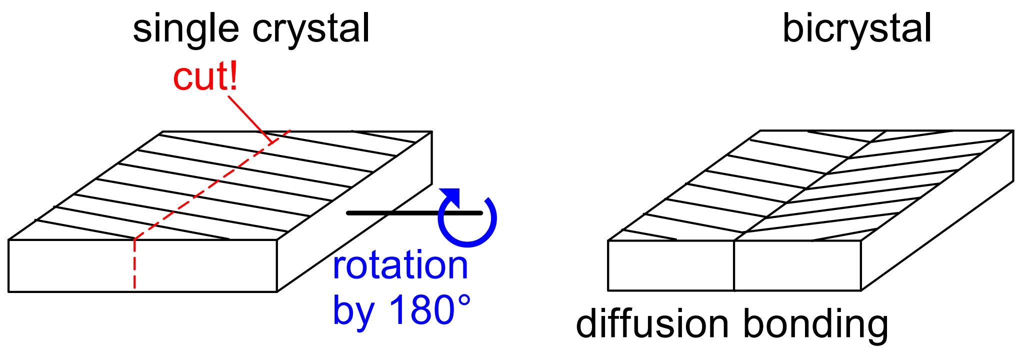

Analysis of Stucture and Composition of GBs

by Q-HRTEM

by Q-AEM (EELS and / or EDS)

Σ3 {111} $(1\bar{1}0)$ GB in $SrTiO_3$

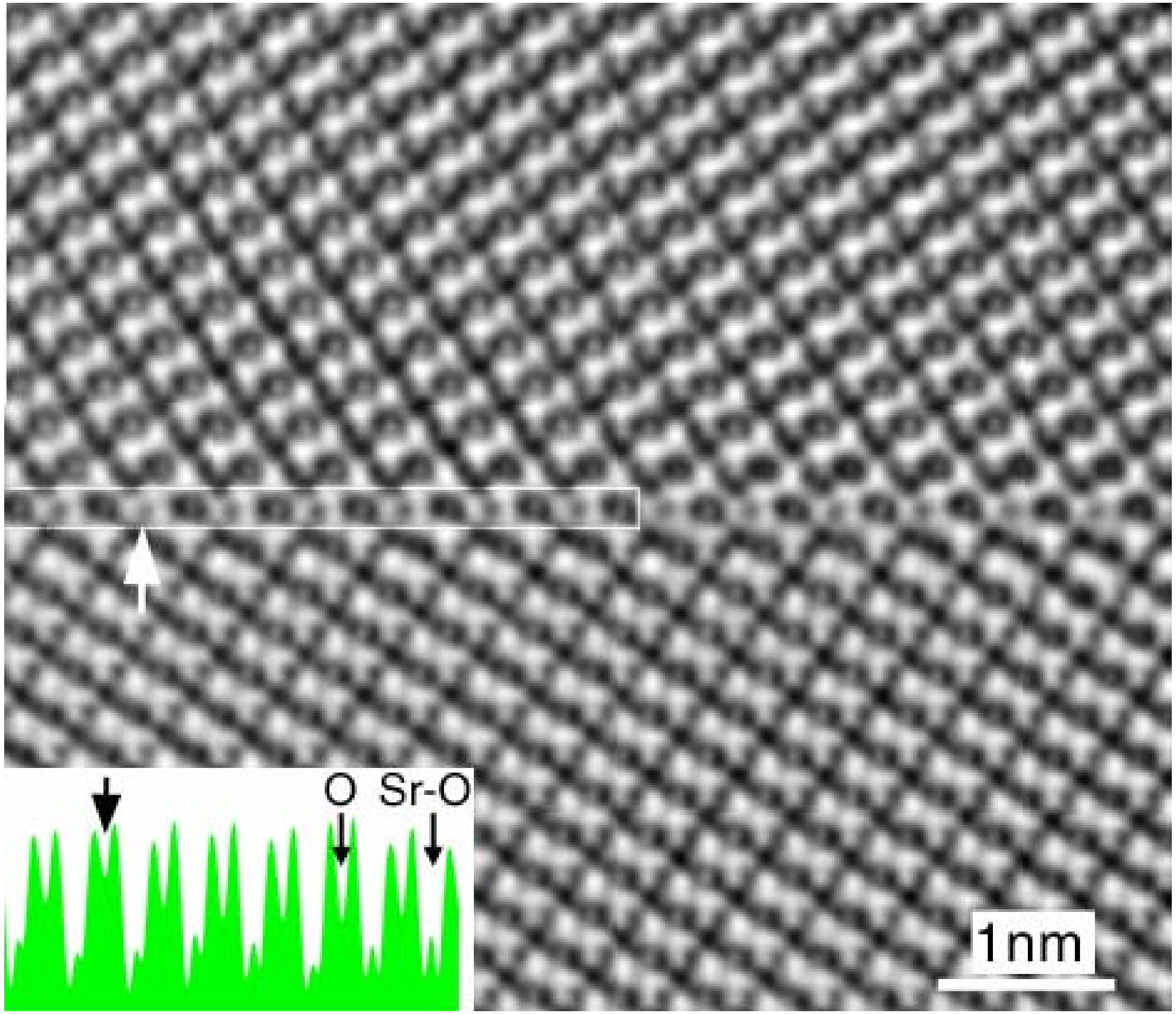

Zhang et al, Science <u>302</u> (2003) 846

Studies at GBs in Bicrystals of STO

HRTEM

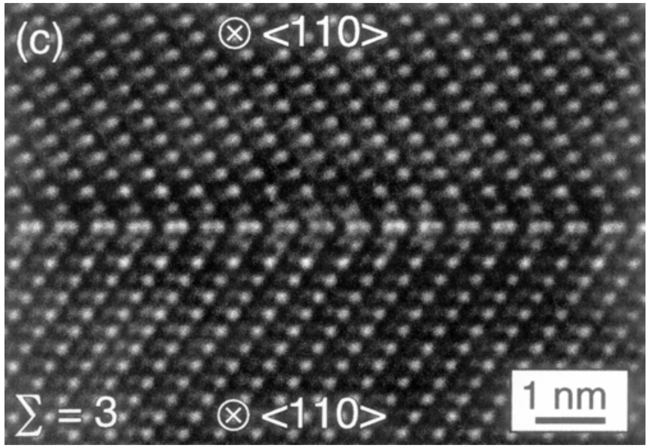

Σ 3 (111) symmetrical twin

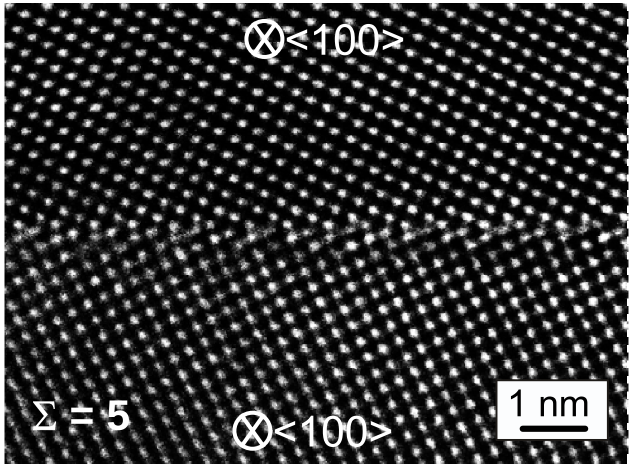

Σ 5 (310)

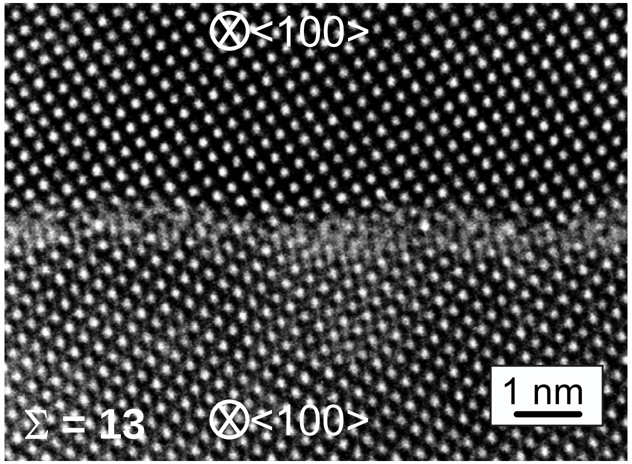

Σ 13 (510)

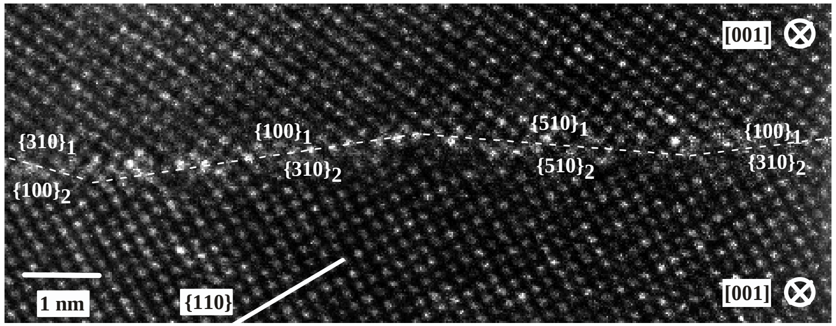

Σ 13 (510), facetted gb

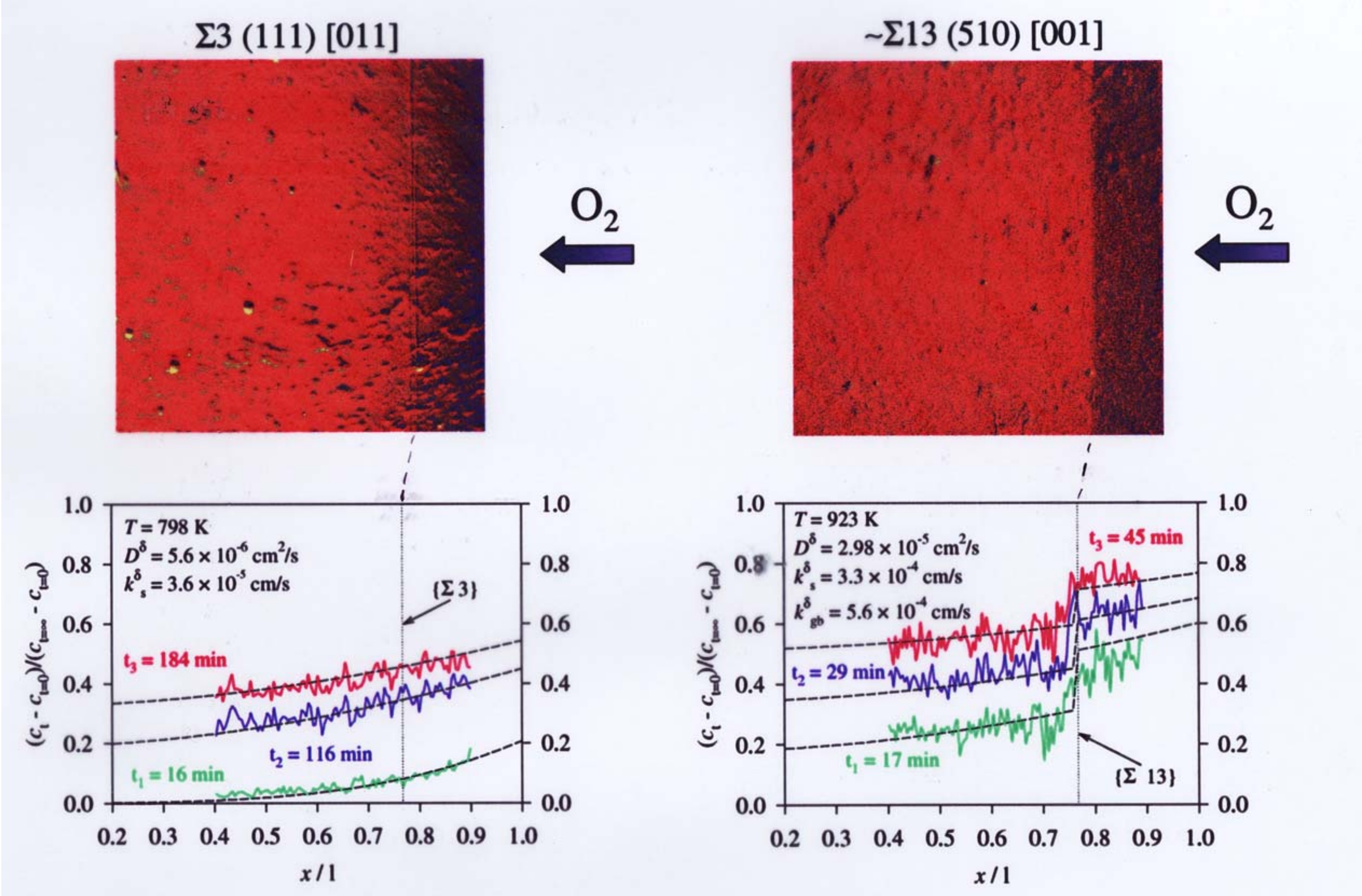

M. Leonhardt, J. Jamnik, J. Maier, Electrochem. and Solid State Lett. 2 [7], (1999), 333

Studies at GBs in Bicrystals

3 D-Information by HRTEM for Σ 5 (103)

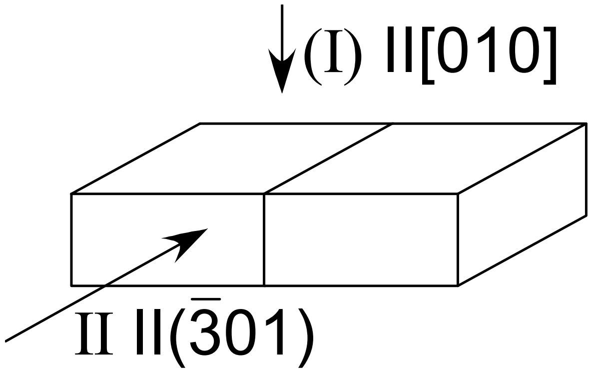

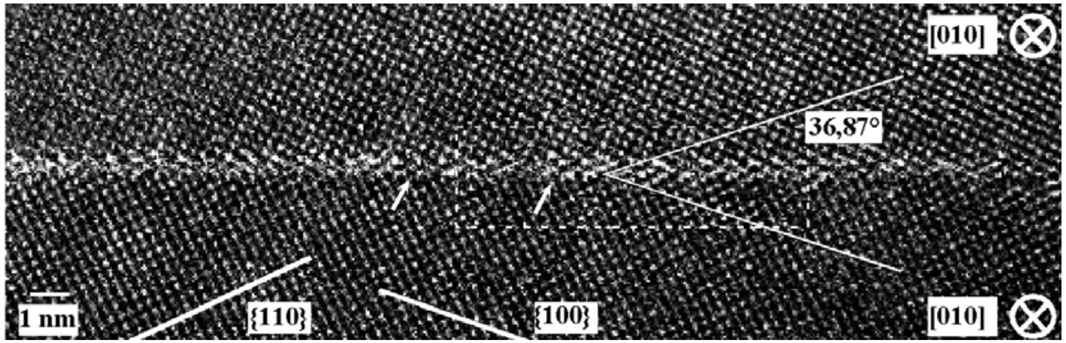

Σ 5 (103) in [010] projection
steps at GB are marked

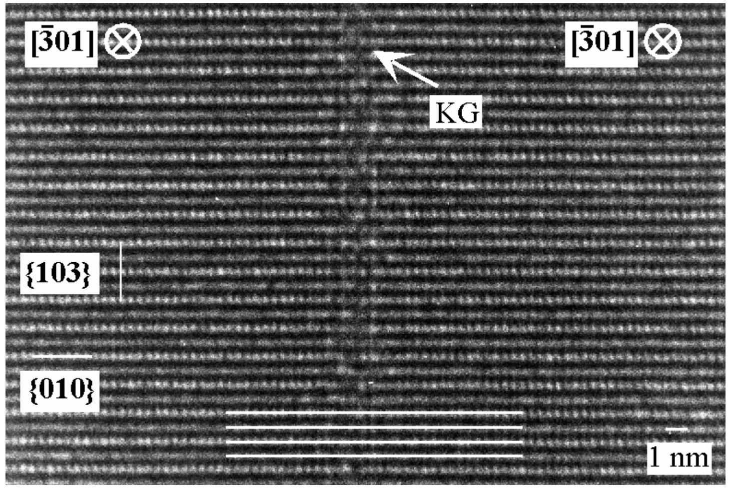

Σ 5 (103) GB in [$\bar{3}$01] projection
no displacement of
2 crystals w. r. t to each other

$SrTiO_3$ Σ=5 (310) [001]

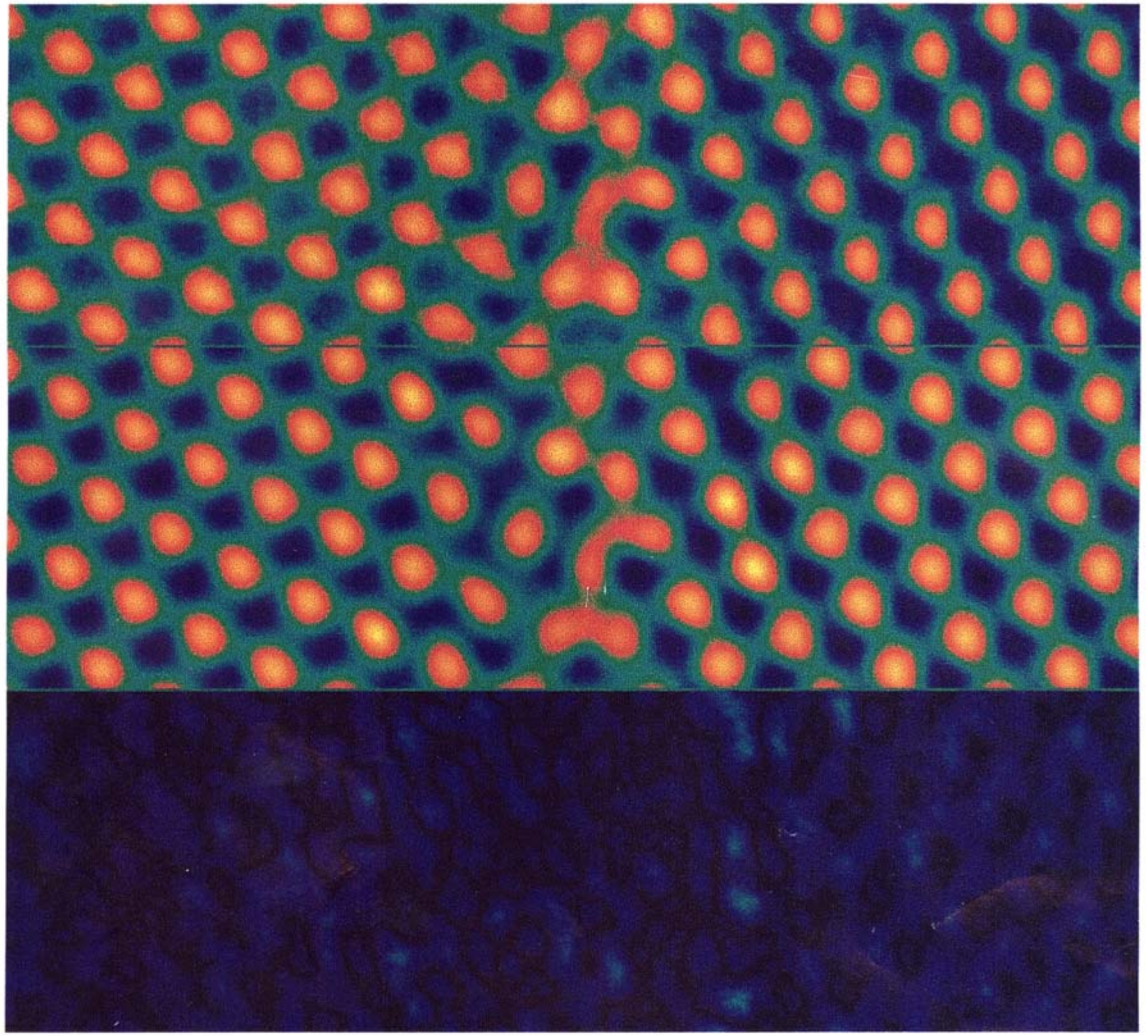

experiment

simulation

difference

CSL-Model 1.57 Å expanded + relaxed

Interfacial Electronic Structure

acquisition of 100 spectra within
25 nm across the GB plane

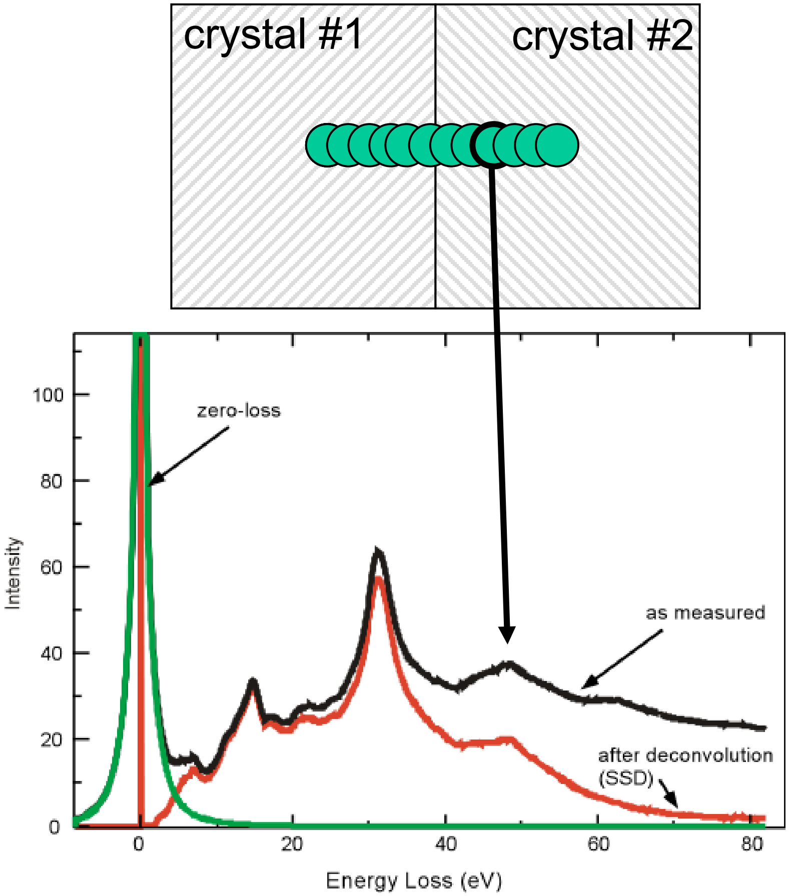

Analysis:

$$ELF(E) \propto \Im\left(\frac{-1}{\varepsilon_1 + i\varepsilon_2}\right)$$

Kramers-Kronig
analysis

$$\Re\left(\frac{-1}{\varepsilon_1 + i\varepsilon_2}\right)$$

$$\varepsilon(E) = \varepsilon_1(E) + i\varepsilon_2(E)$$

$$J_{cv} = J_{cv_1} + iJ_{cv_2}$$
$$= const \cdot i\left(\varepsilon_2(E) + i\varepsilon_1(E)\right) \cdot E^2$$

$\Re(J_{cv})$: Interband transition strength

Interfacial Electronic Structure and Hamaker constant of GB

VEELS Studies

3 D Representation of Interband Transition Strengh

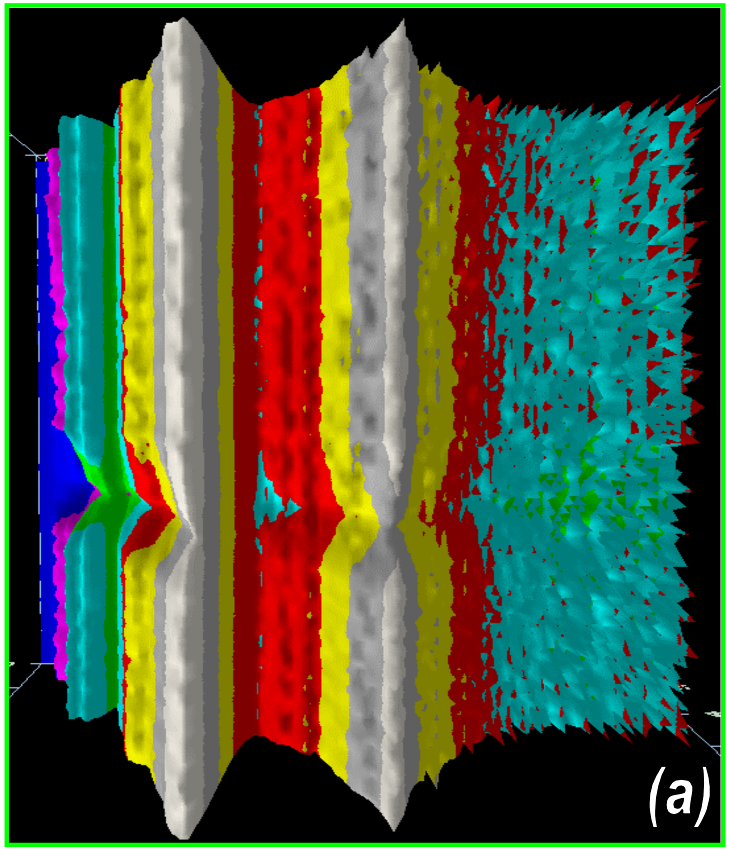

Σ5

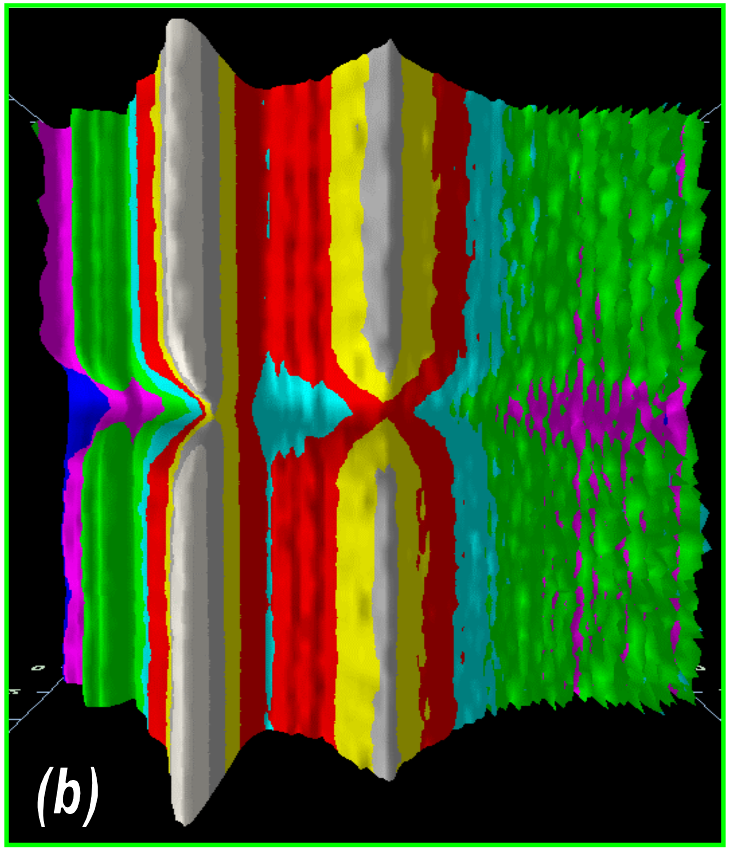

Σ13

Interfacial Electronic Structure

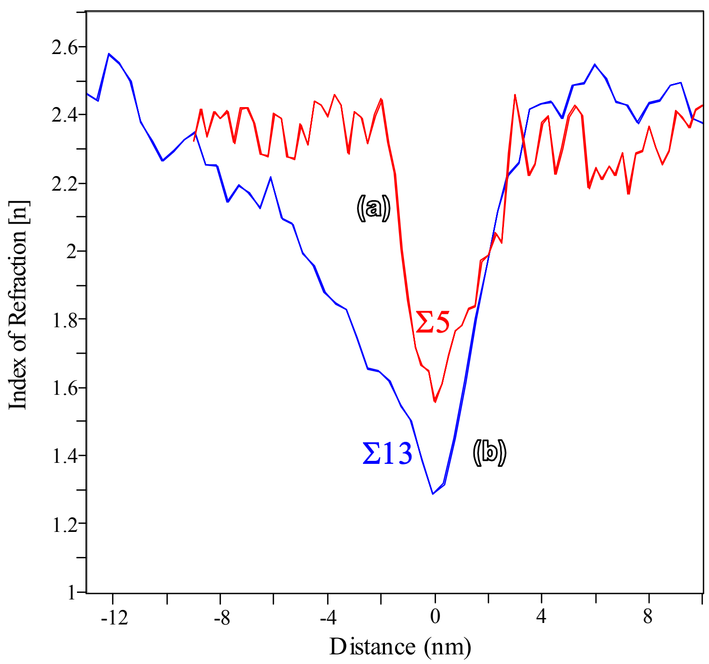

Interfacial Index of Refraction

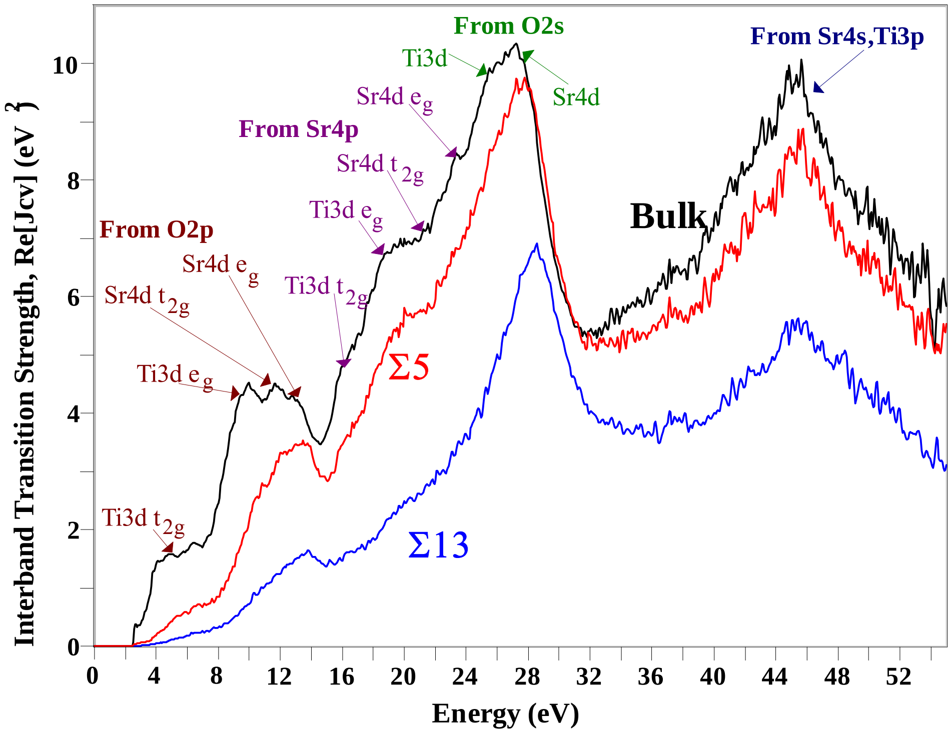

Interband Transition Strength
Bulk STO, Σ5 gb, Σ13 gb

Hamaker Constant of GB

Modelling Hamaker Constant from Atomistic Results

→ Transition to continuum model with different zones

Different Models

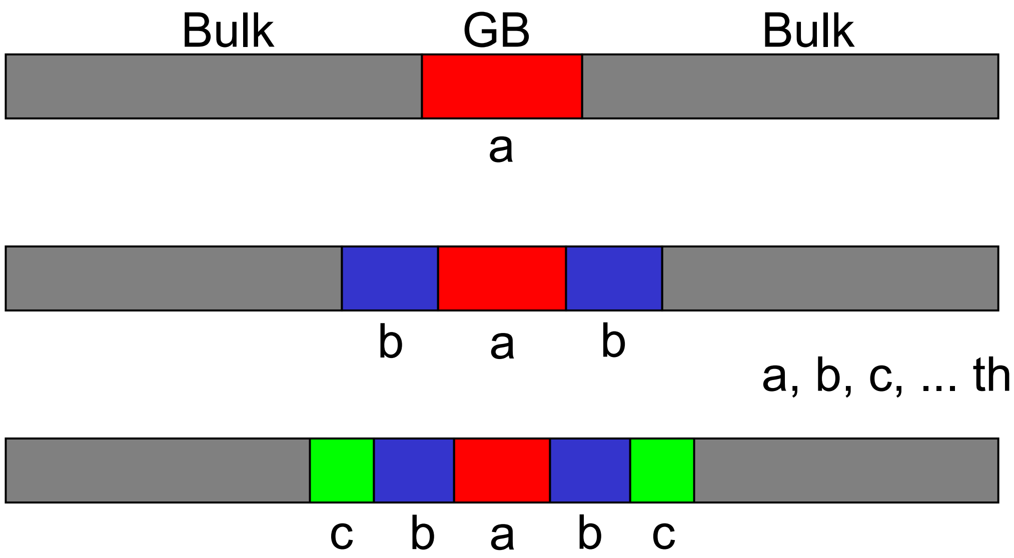

a, b, c, ... thicknesses of layers

Calculation of Retarded Hamaker Coefficient

Grain Boundary Energies for Different Misorientations

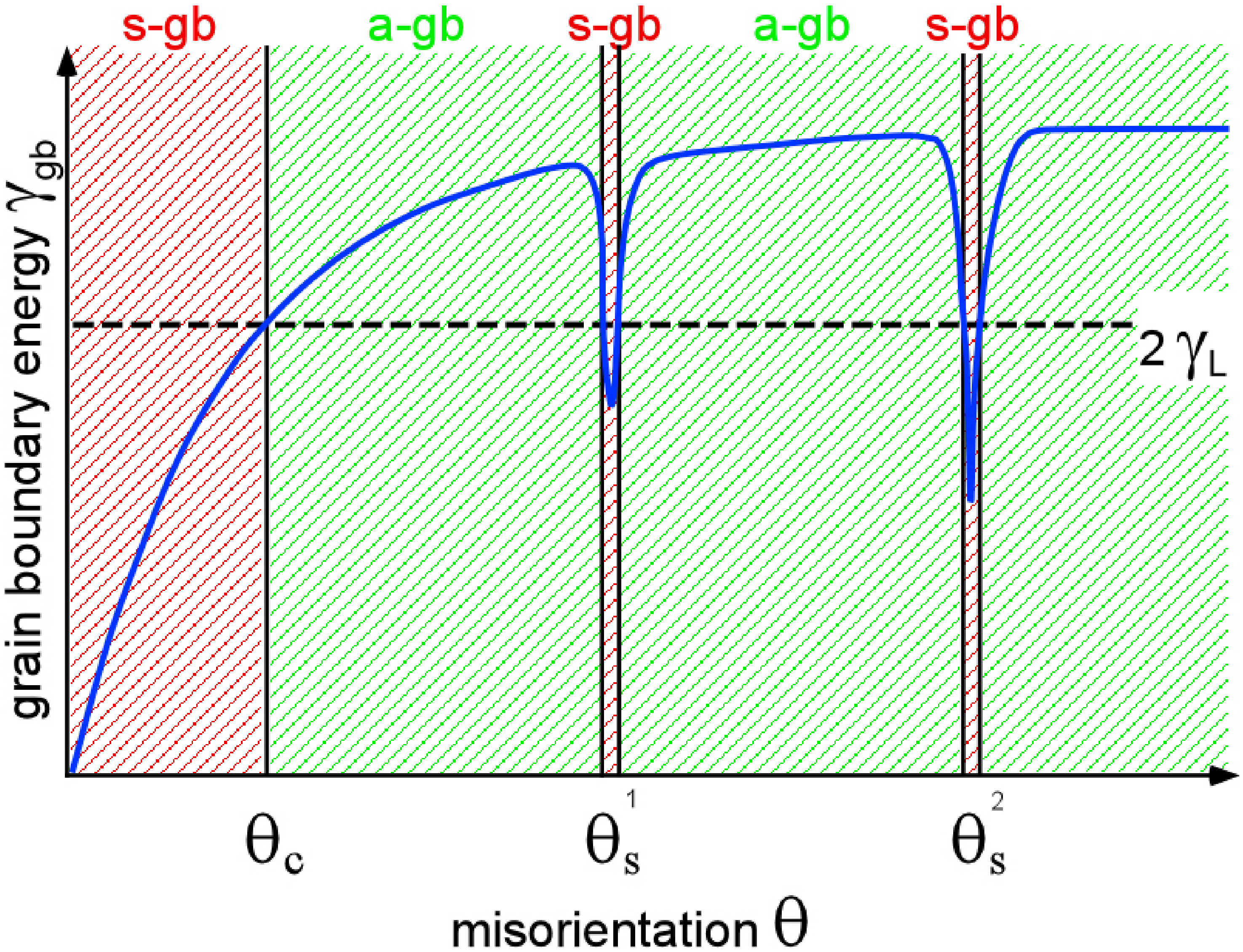

Small-Angle Grain Boundary

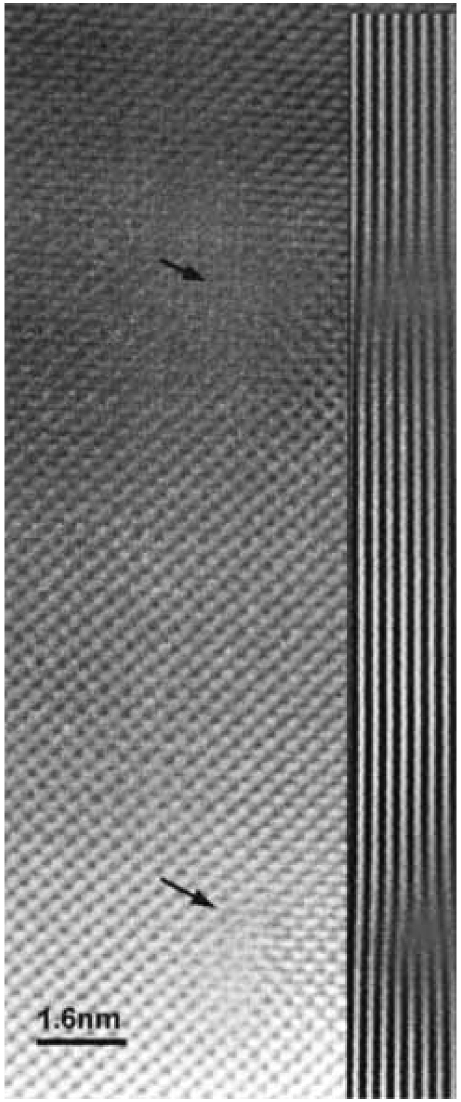

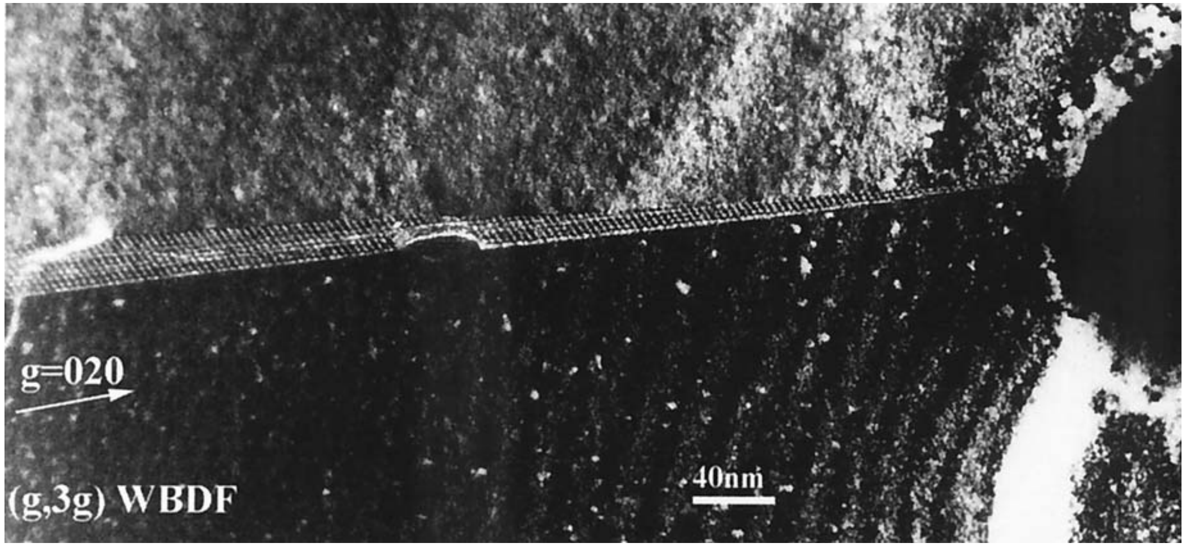

R. A. De Souza et al

Small-Angle Grain Boundary in STO

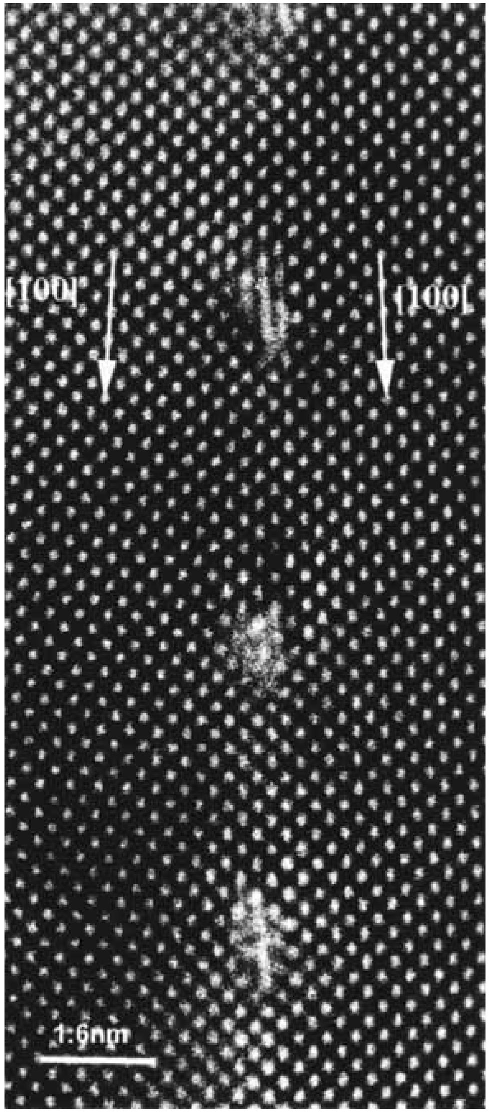

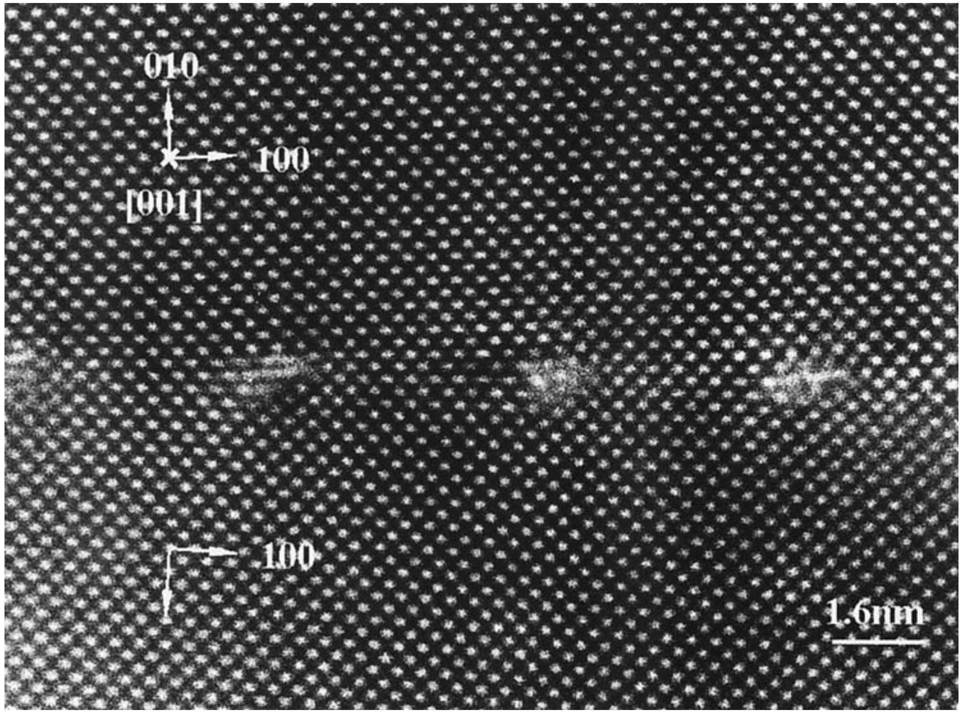

R. A. De Souza et al

Small-Angle Grain Boundary in STO

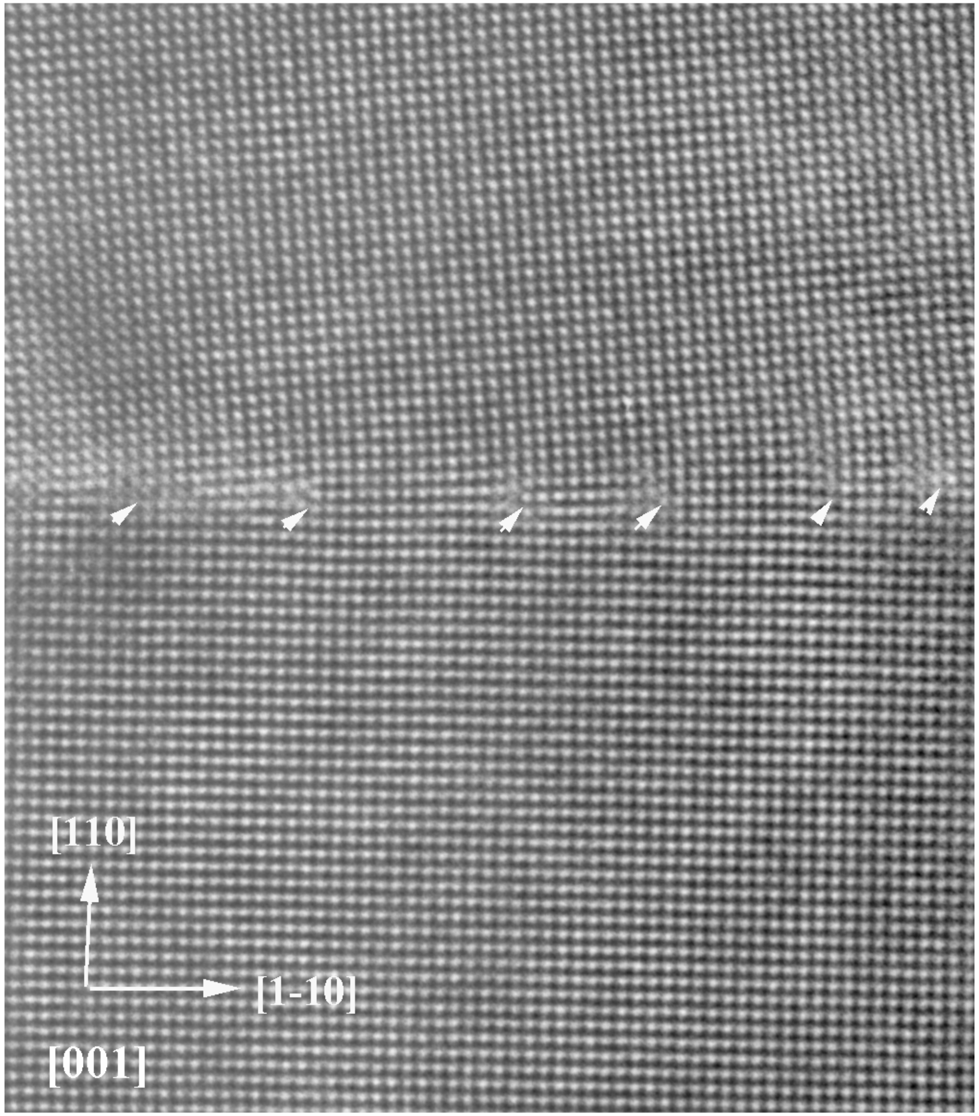

Z. Zhang et al

Composition Close to Dislocations

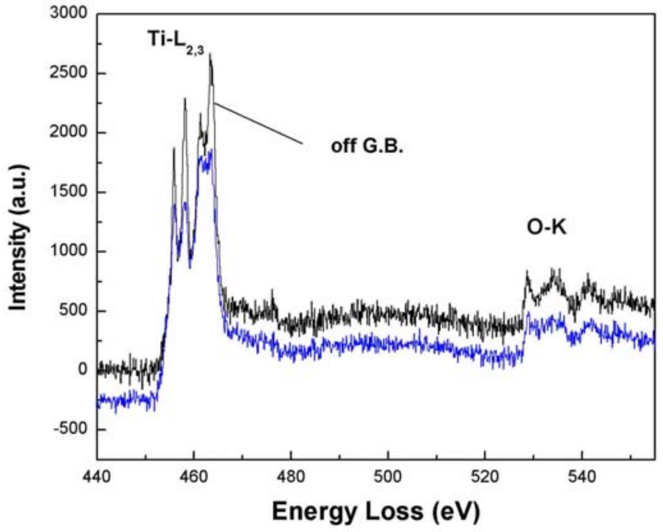

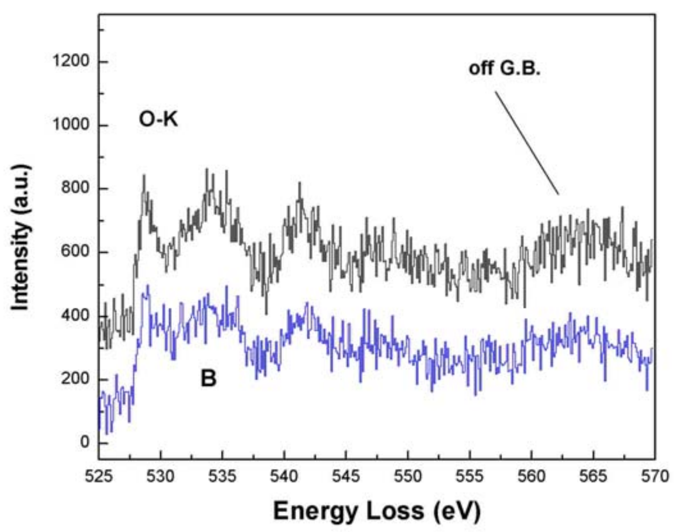

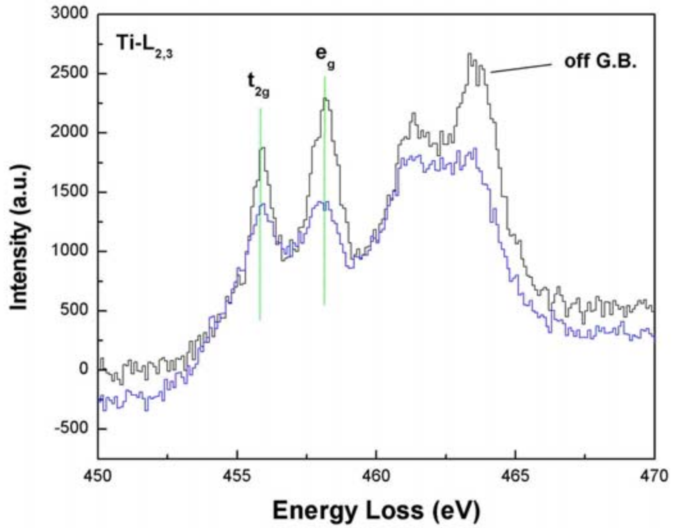

Z. Zhang et al

Composition Close to Grain Boundary

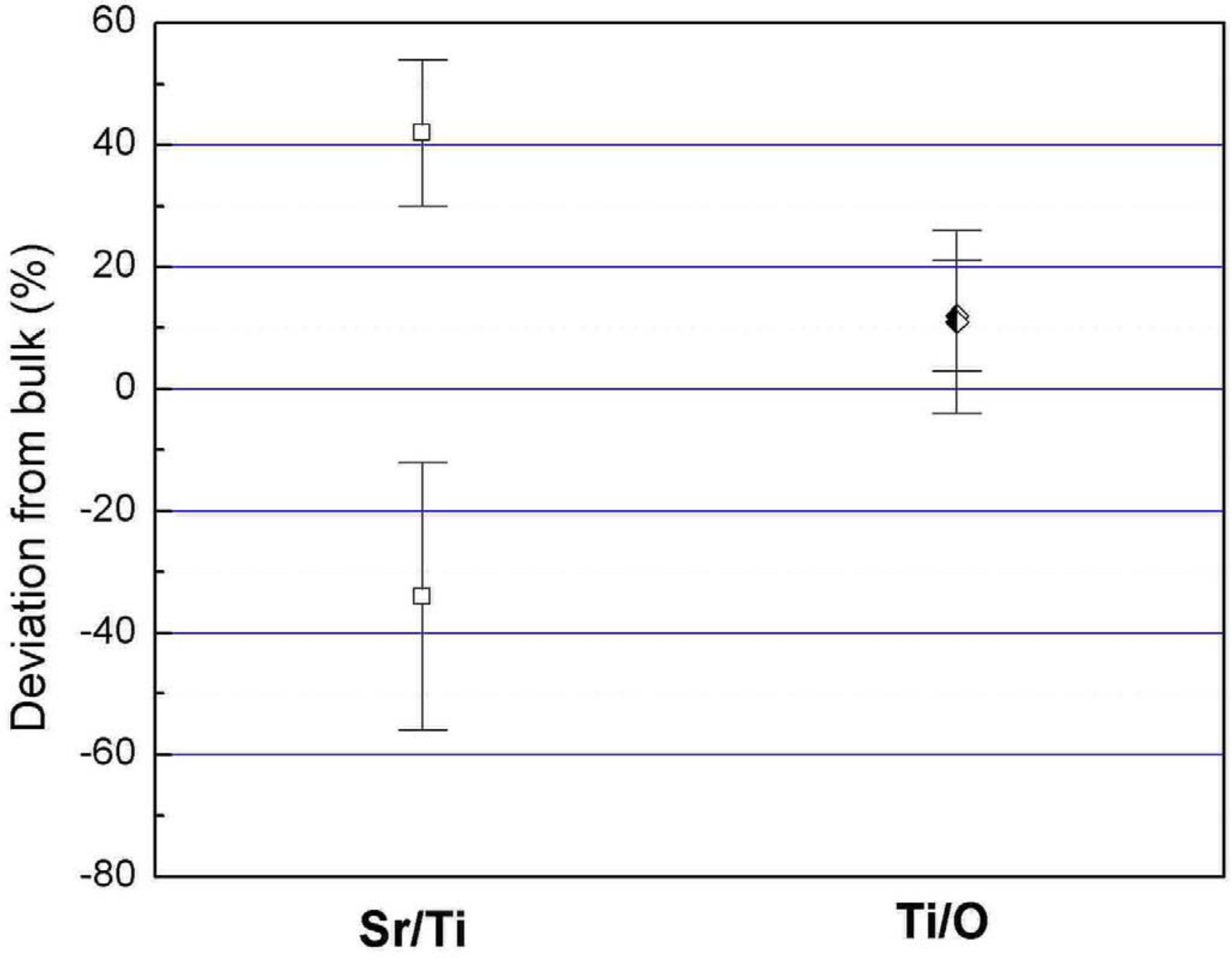

Z. Zhang et al

Small-Angle Grain Boundary

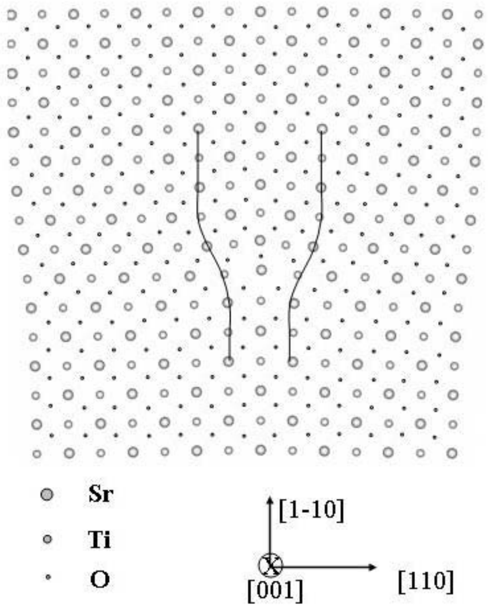

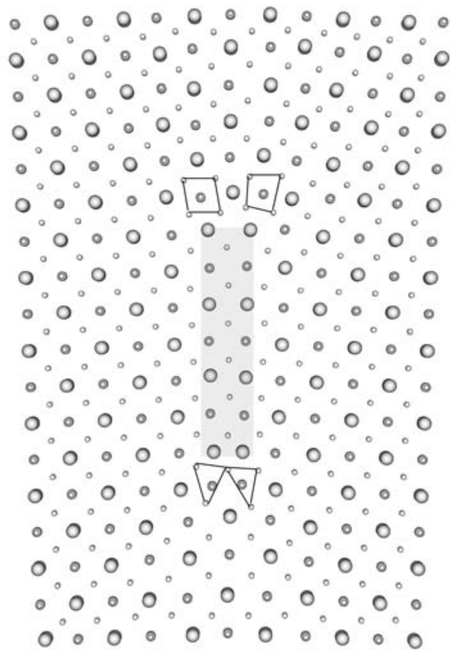

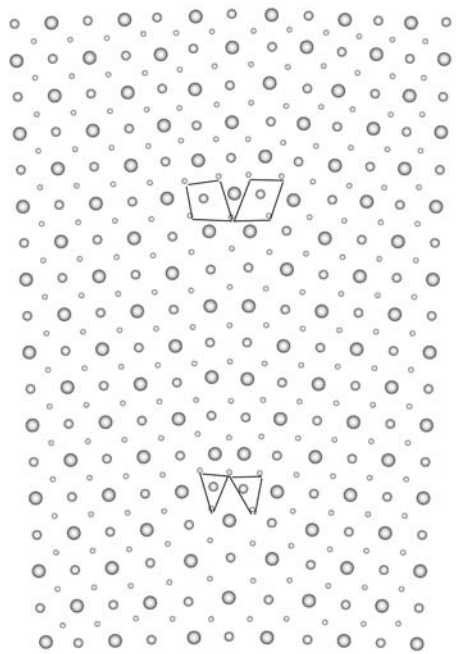

Z. Zhang et al

Conductivity of Small-Angle Grain Boundary

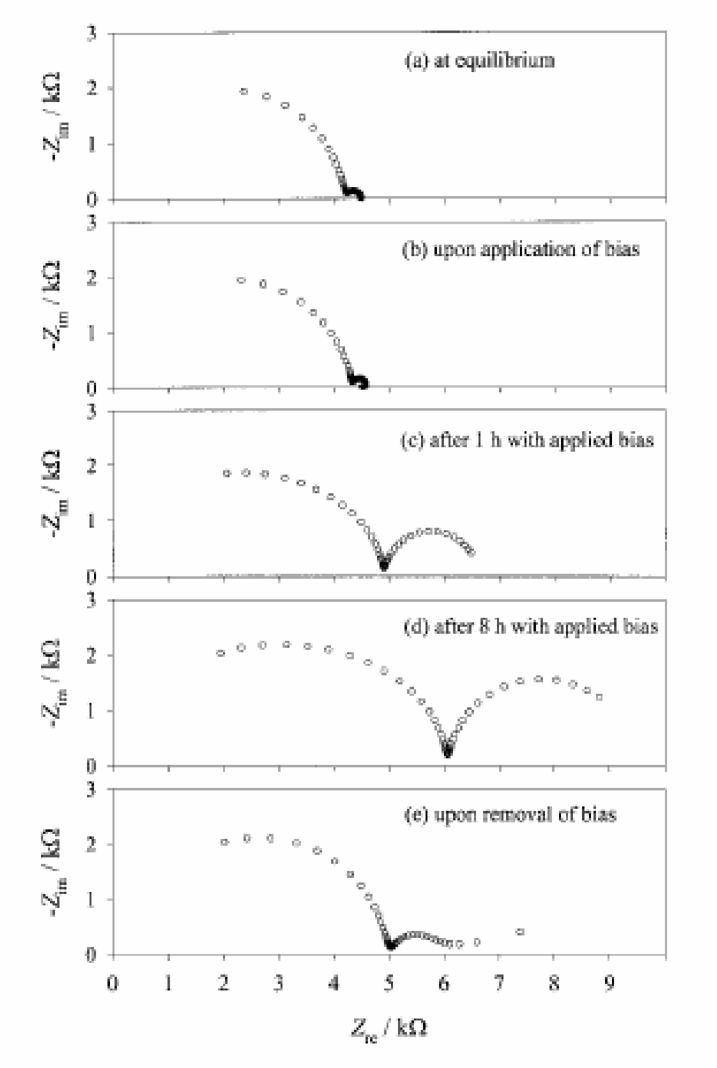

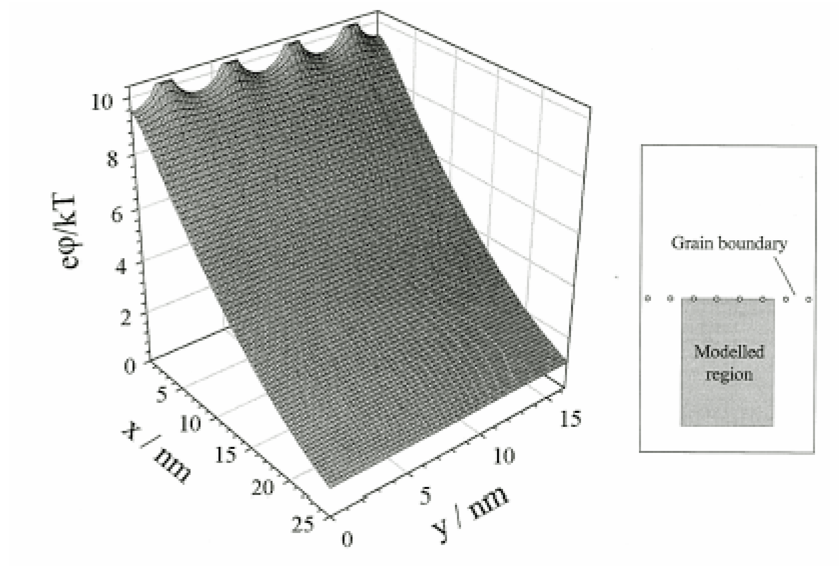

R. A. De Souza et al

Small-Angle Grain Boundaries

UHV diffusion bonding at 1700K
(W. Kurtz)

Tilt GB

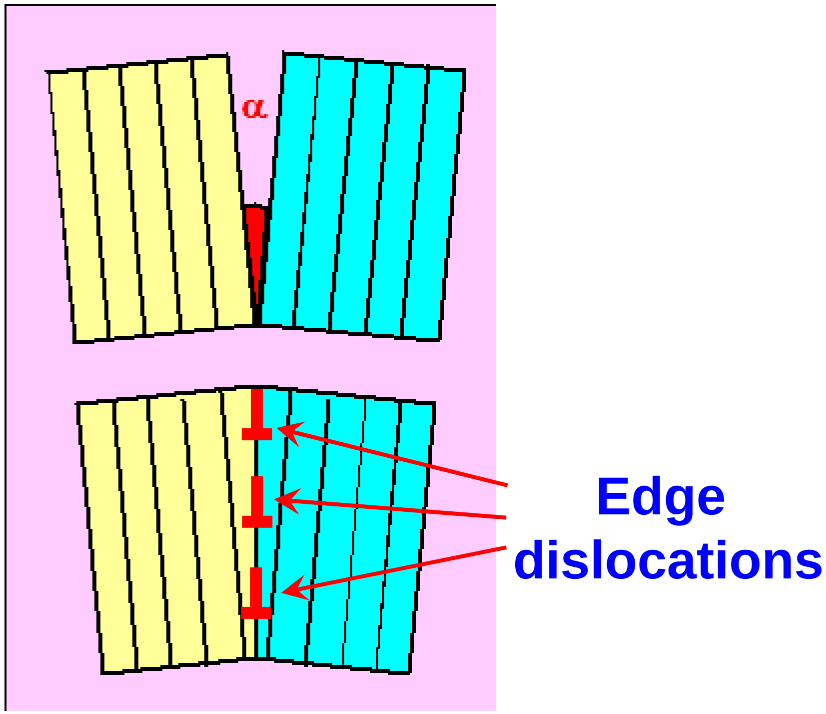

Twist GB

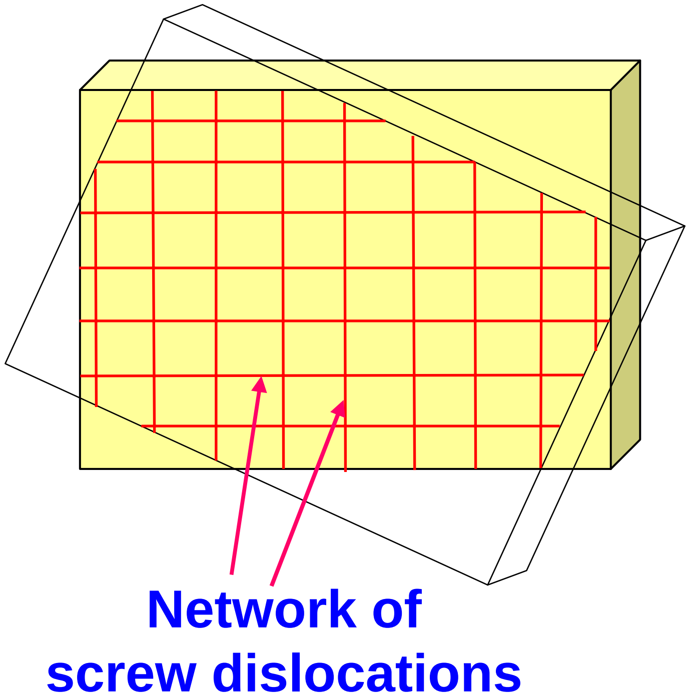

<110> core

HRTEM Image (*Bicrystal; 1700 K*)

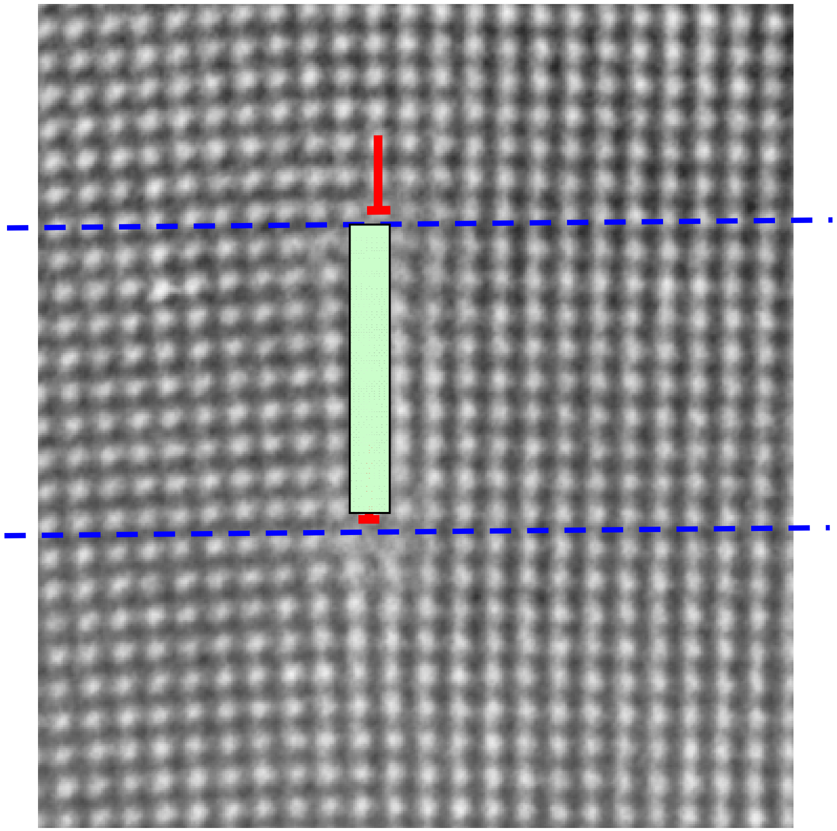

W. Sigle, Z. Zhang Phys. Rev. **B 66** (2002) 214112

<110> core

Forces Between Two Partial Dislocations

Forces favour climb dissociation !

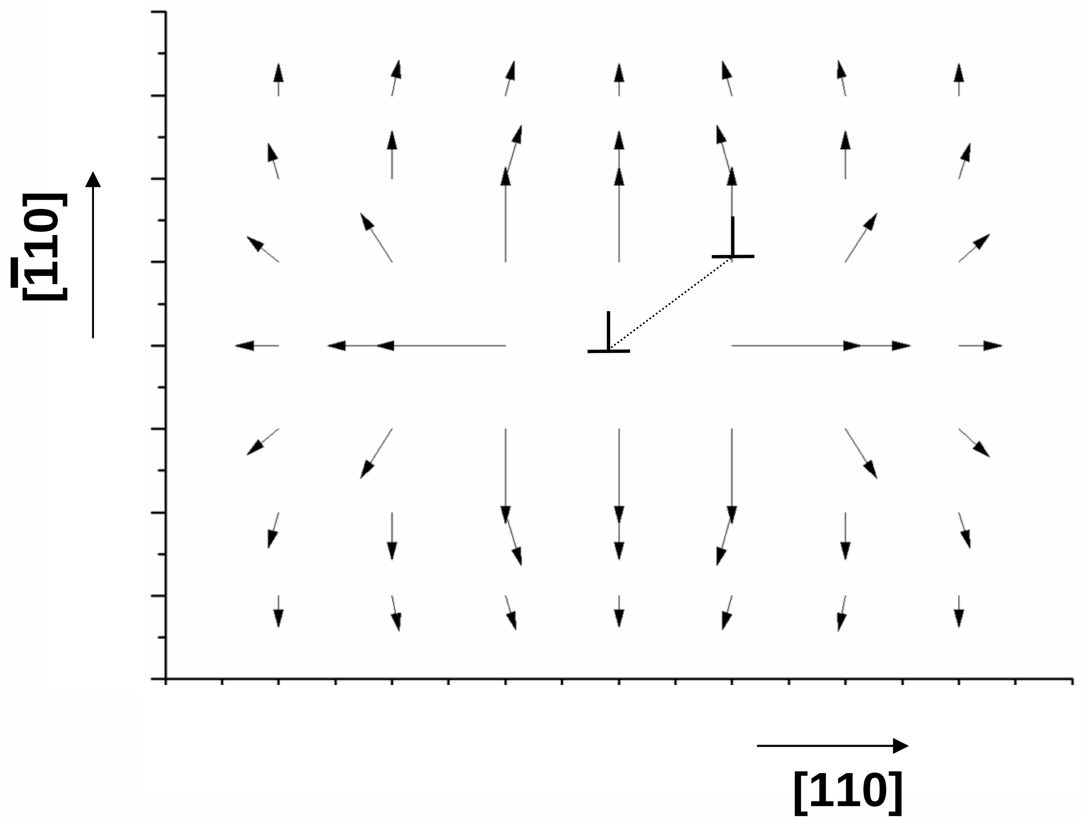

<110> core

HRTEM Image (*Bicrystal; 1700 K*)

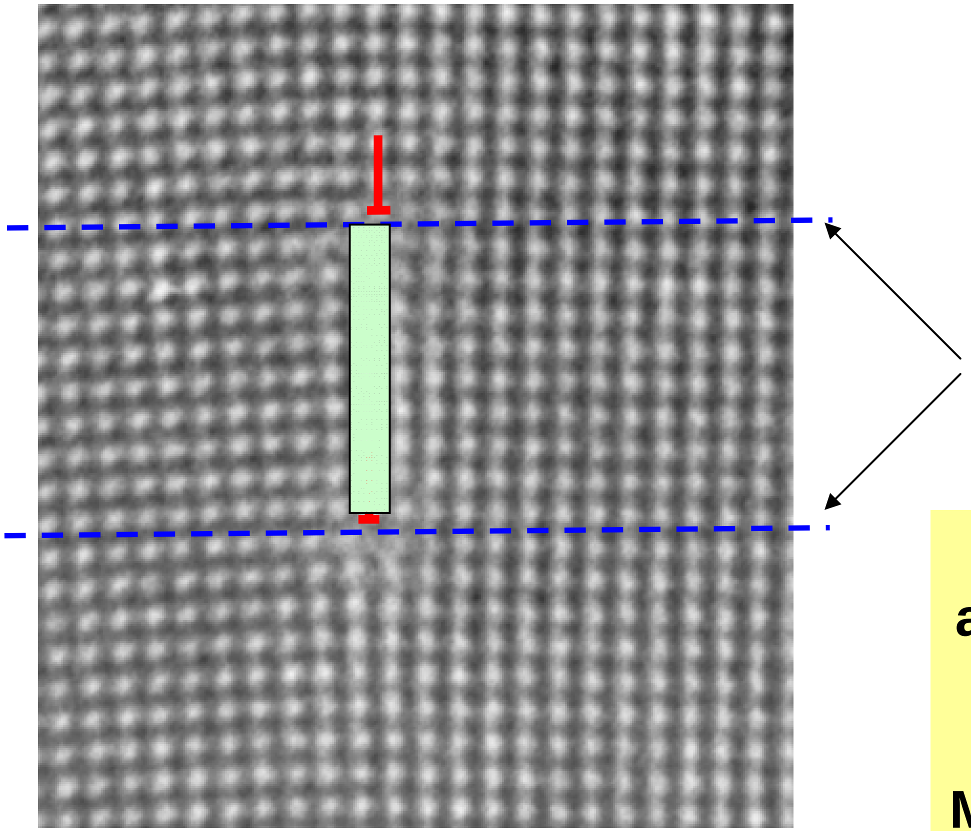

Climb dissociation at elevated temperatures

⇩

Movement only thermally activated

W. Sigle, Z. Zhang Phys. Rev. **B 66** (2002) 214112

<100> core

a<100>{100} Edge Dislocation Core

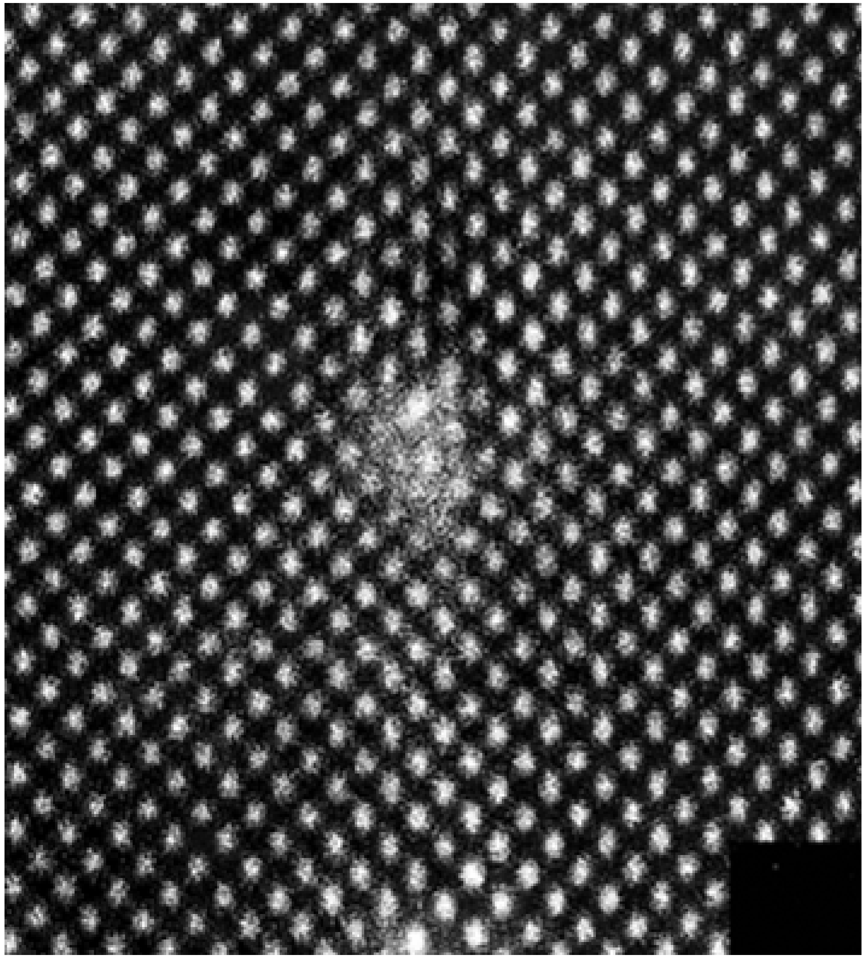

W. Sigle, Z. Zhang Phys. Rev. **B 66** (2002) 094108

a<100> edge core

Atomistic Model of Dislocation

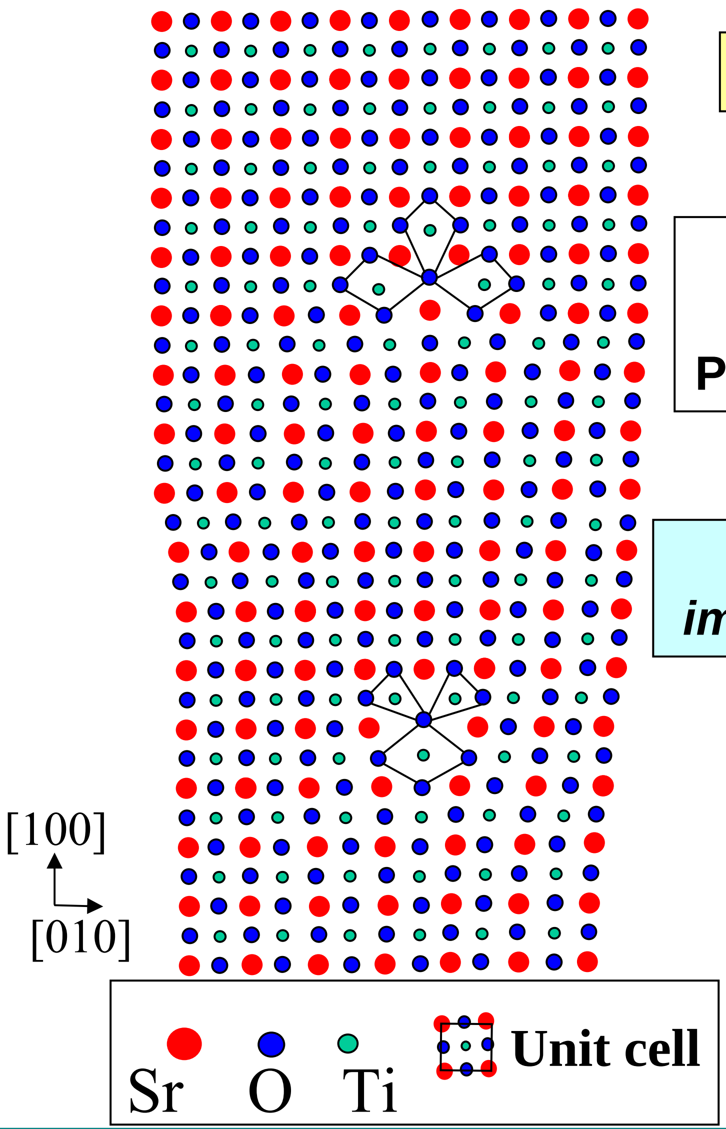

Removal of O atoms

Distorted Ti-O polyhedra

Increased Ti:O ratio

Positively charged core

Reduced crystal field

In agreement with impedance spectroscopy

R. de Souza, J. Maier
MPI-FKF

Explains Ti-$L_{2,3}$ edge

Larger Sr-O separations

Explains O-K edge

W. Sigle, Z. Zhang

a<100> Screw Dislocation

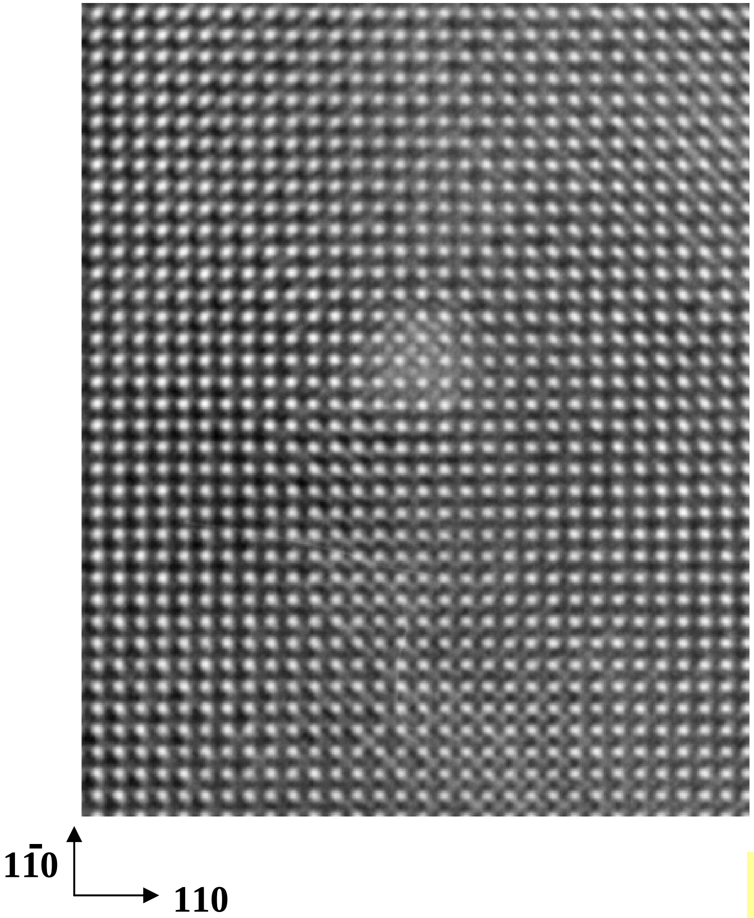

Atom displacement map

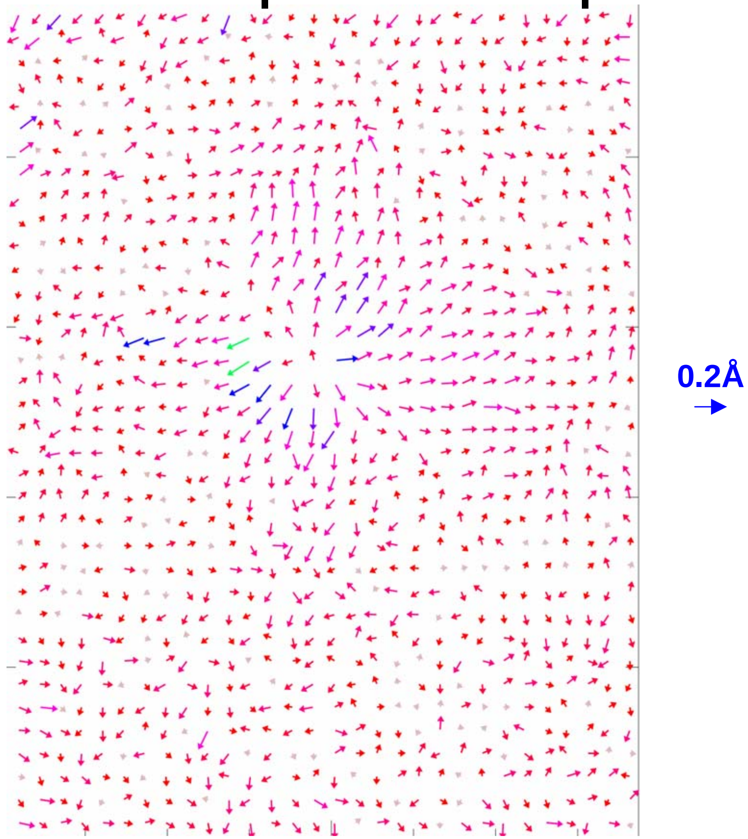

Expansion within the core
Stronger along <110> than along <100>
"Non-planar dissociation"
(Influence on plasticity?)

a<100> screw core

Chemistry with (nearly) Atomistic Resolution

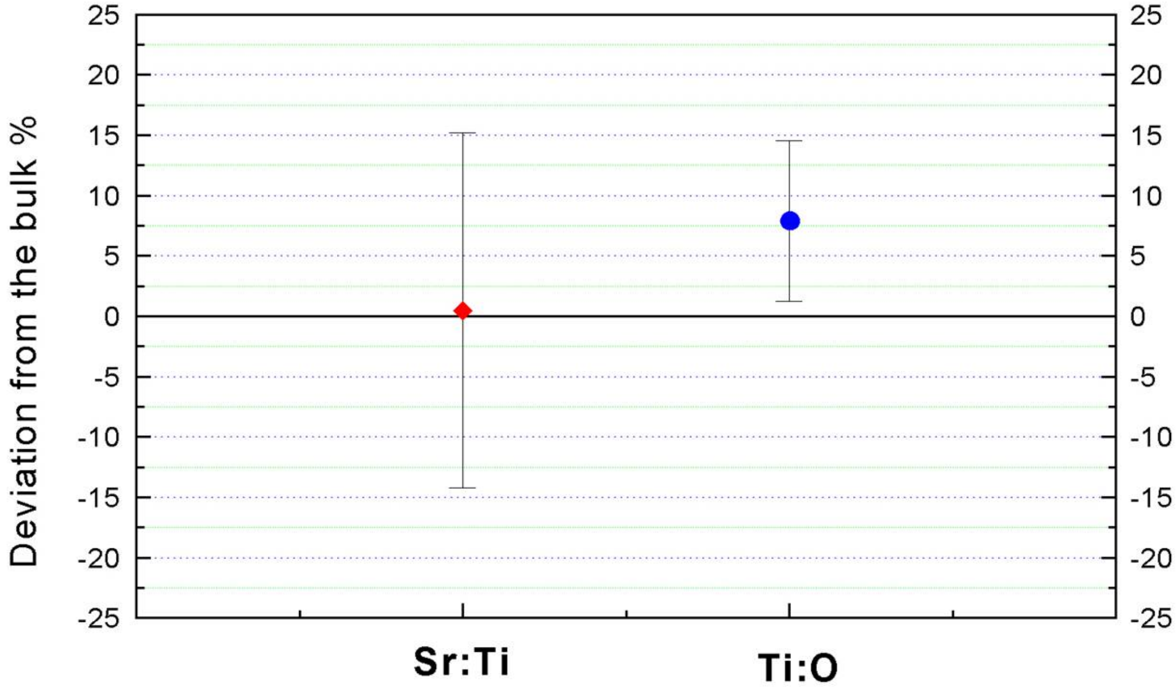

- **In the dislocation core higher Ti/O ratio than in the bulk (*oxygen deficiency)***

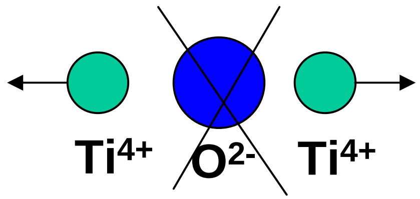

Repulsion of Ti ions ⟶ “expansion”

Crystal Field Effect on Ti 3d Levels

Octahedral ligand field

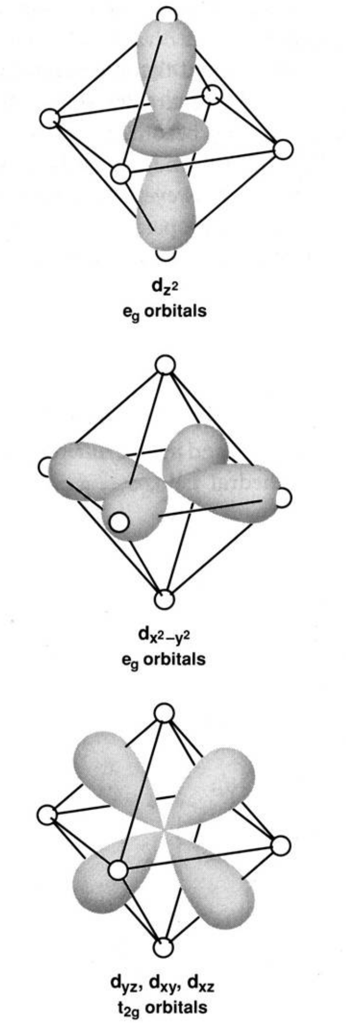

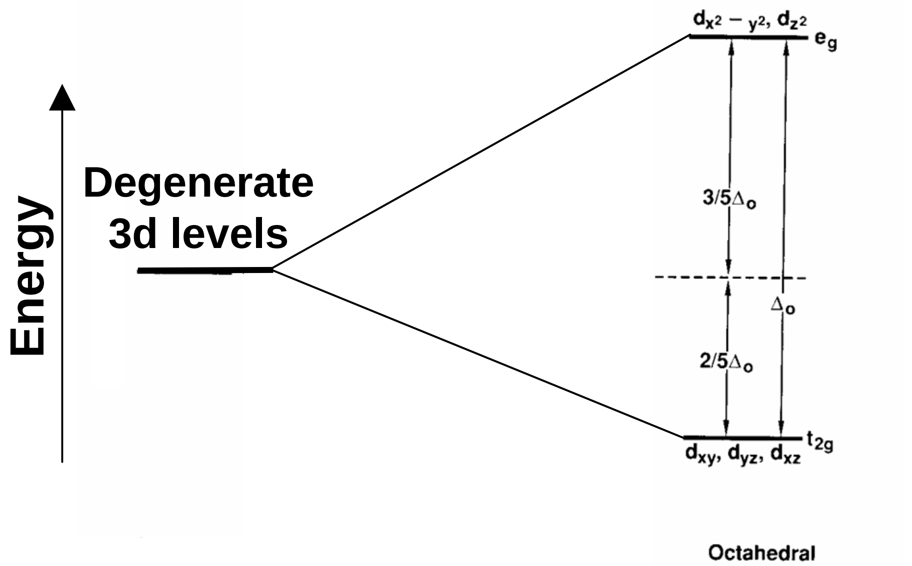

Crystal field splitting

influence on fine structure of energy loss edges

Edge Dislocation

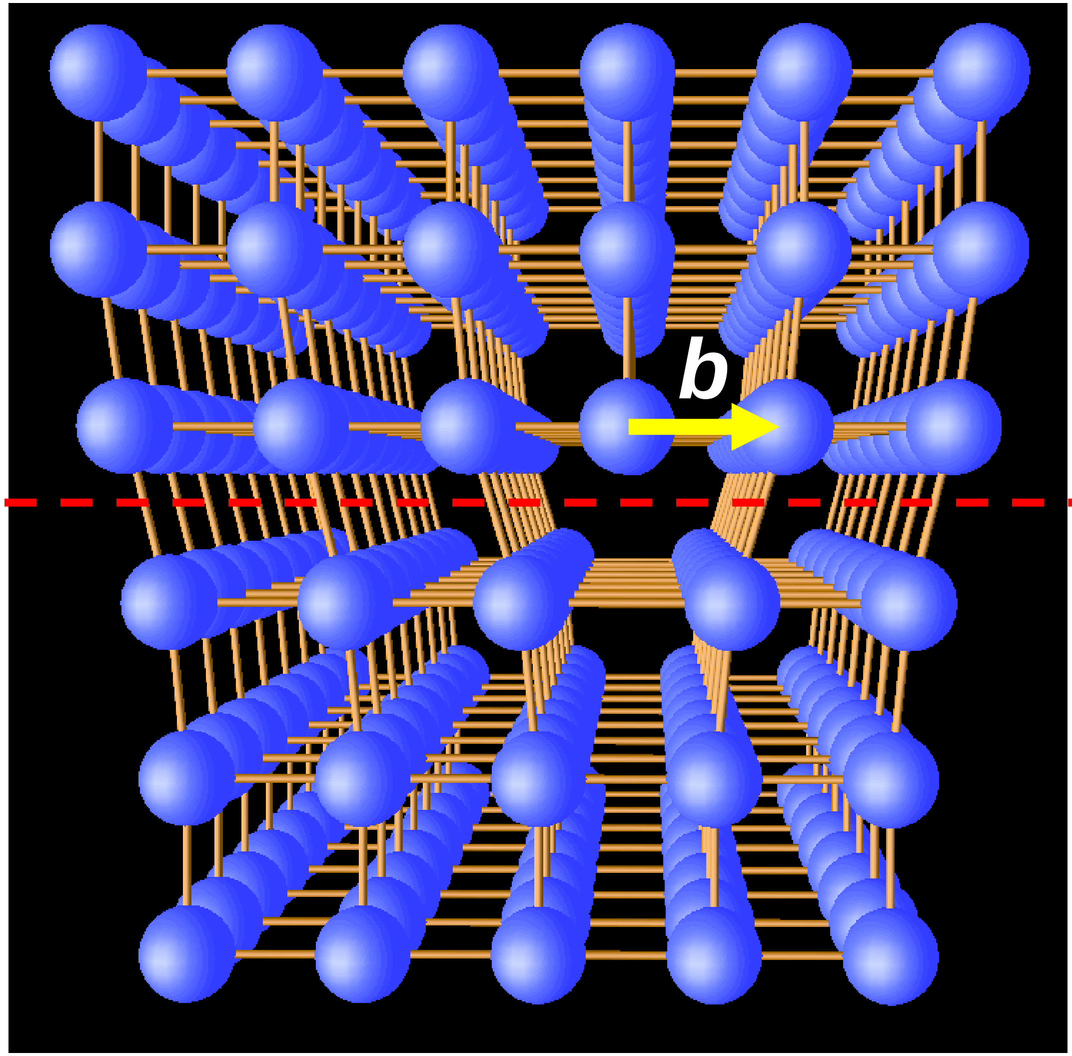

Burgers vector *b*

Slip plane

Possible Burgers Vectors in $SrTiO_3$

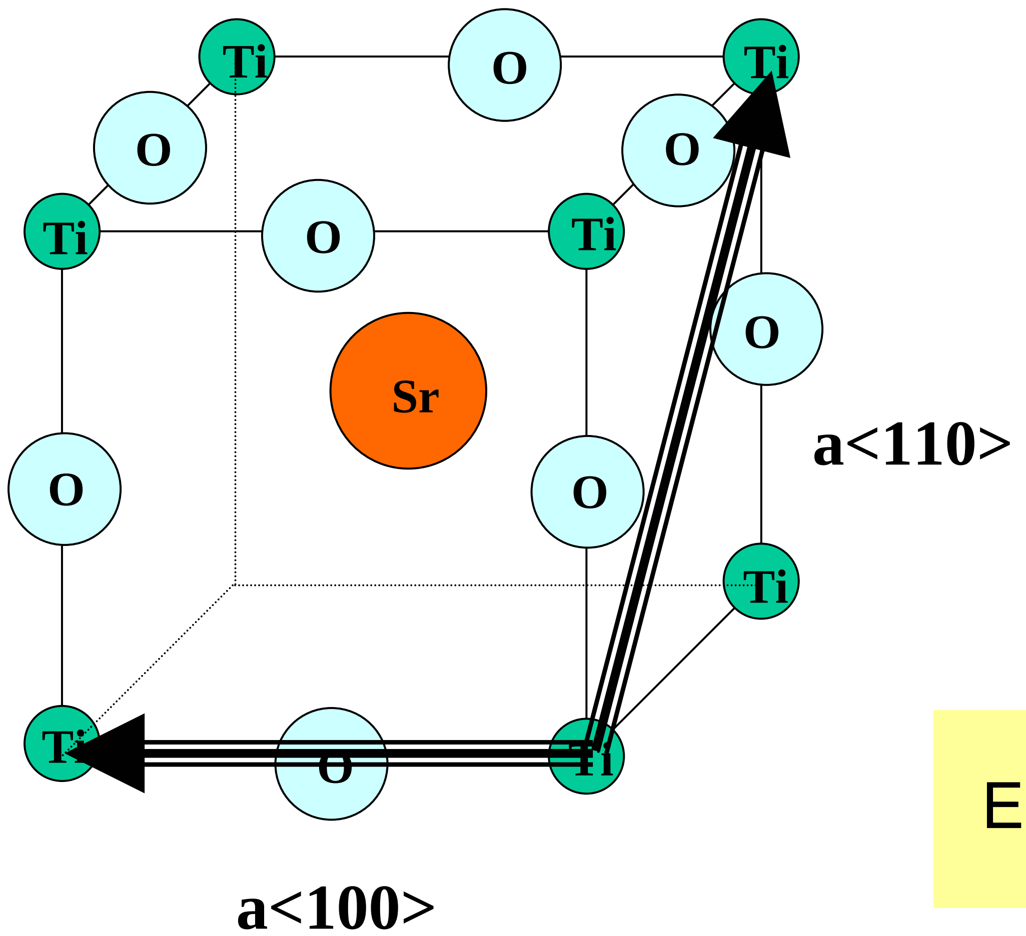

$$E \sim \frac{1}{2} G b^2$$

D. Brunner, W. Sigle, S. Taeri, JACS, Z. Metallkunde

Heterophase Boundaries M/$SrTiO_3$

lattice mismatch

Sc	Ti	V	Cr	Mn	Fe	Co	Ni	Cu	Zn
Y	Zr	Nb	Mo	Tc	Ru	Rh	Pd	Ag	Cd
La	Hf	Ta	W	Re	Os	Ir	Pt	Au	Hg

electronegativity

Sc	Ti	V	Cr	Mn	Fe	Co	Ni	Cu	Zn
Y	Zr	Nb	Mo	Tc	Ru	Rh	Pd	Ag	Cd
La	Hf	Ta	W	Re	Os	Ir	Pt	Au	Hg

Difference to $SrTiO_3$:

blue:	big	> 5%
red:	small	≤ 5%
green:	good matching	≤ 1%

bcc: **Cr**, Mo

fcc: **Ni**, **Pd**

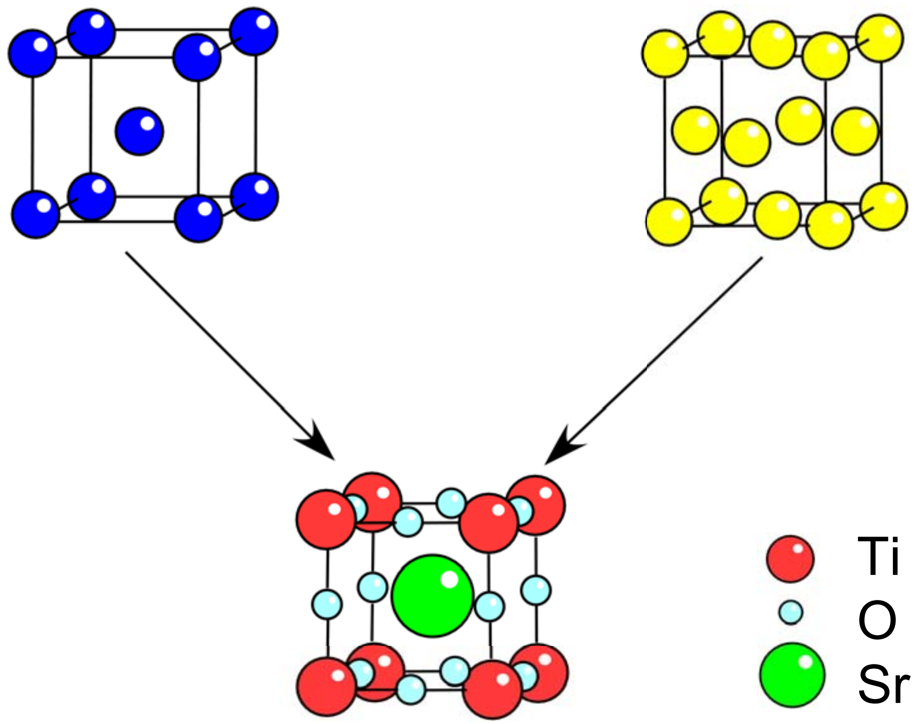

Structural Studies for Pd/Al_2O_3 Interface

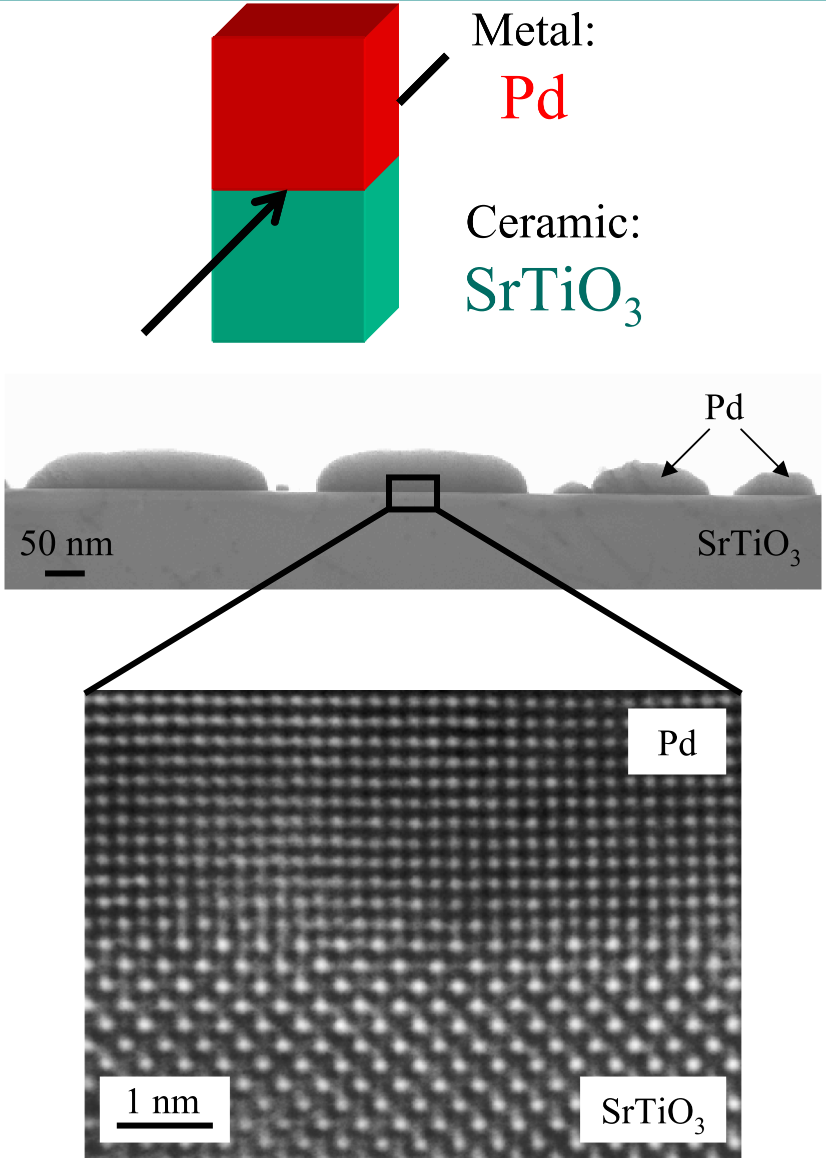

➡ Specimen preparation:

Molecular Beam Epitaxy (MBE)

➡ Orientation relationship investigations:

Conventional Transmission Electron Microscopy (CTEM)

➡ Atomic structure of the interface:

High-resolution TEM (HRTEM), Quantitative HRTEM (QHRTEM)

Introduction: Possible positioning of Pd on top of $SrTiO_3$

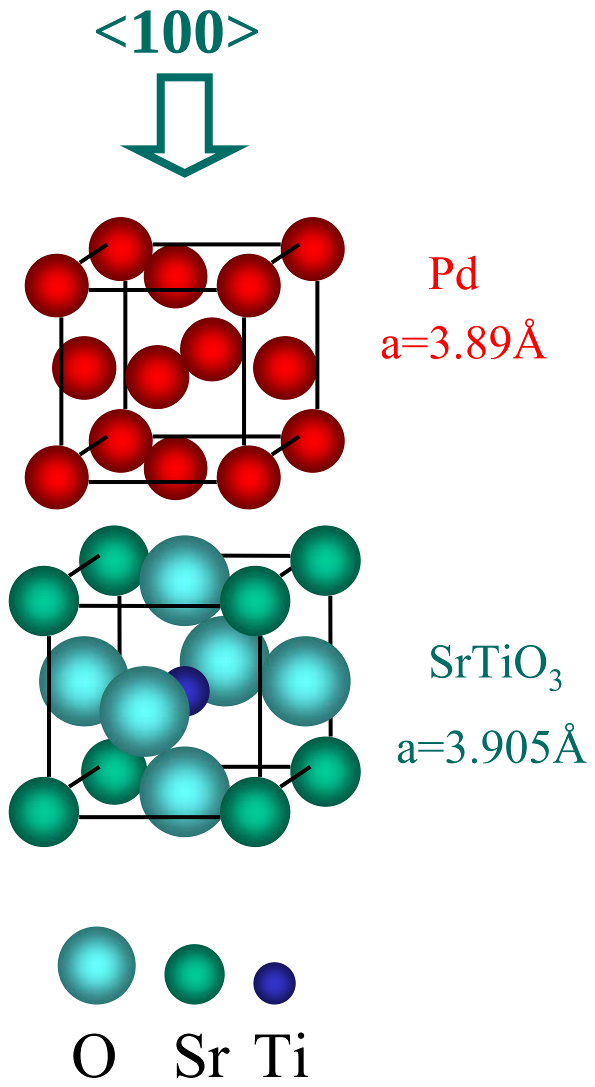

Top view:

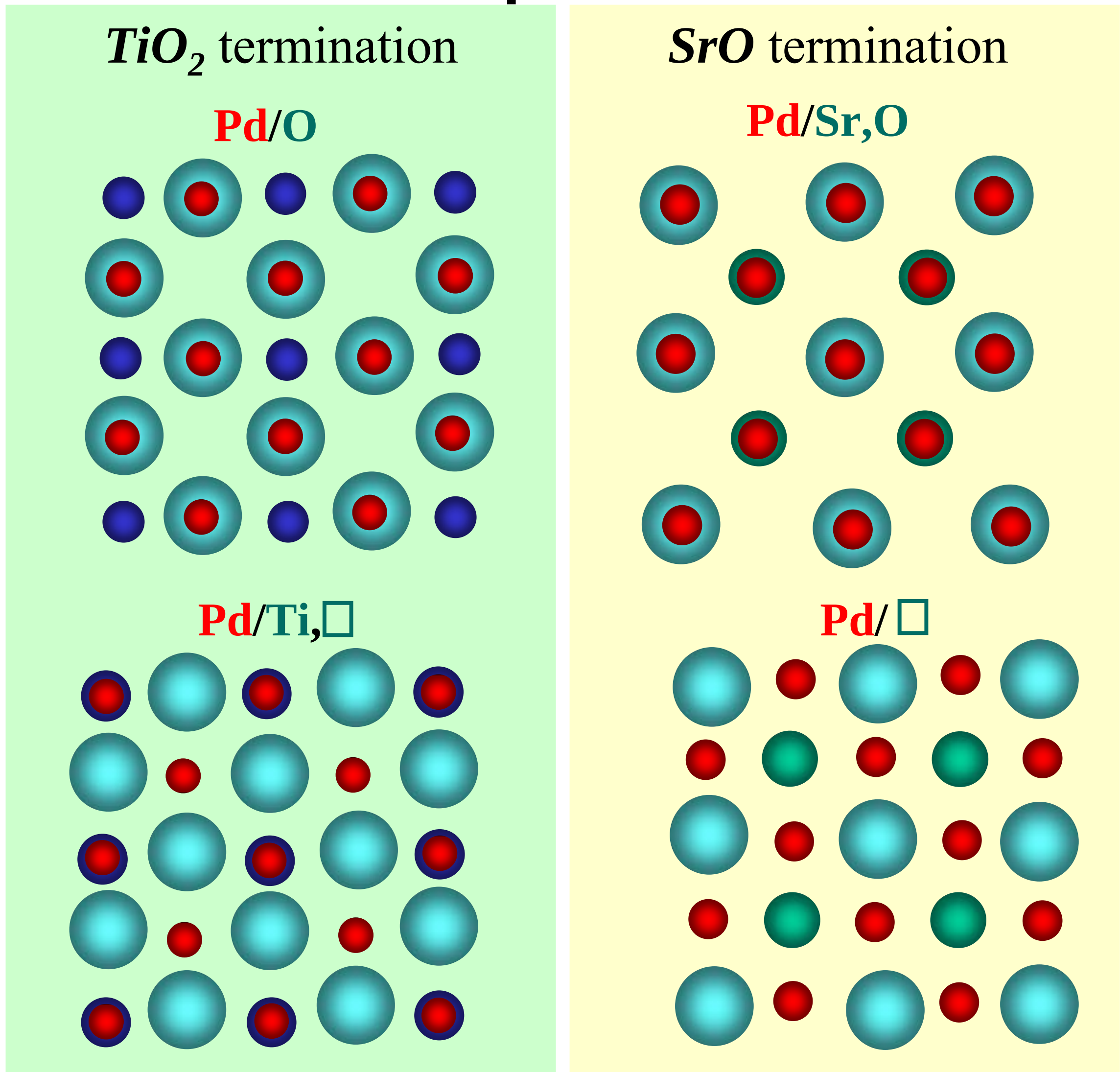

Tomography of Pd/$SrTiO_3$ Interface

<100>

Viewing direction

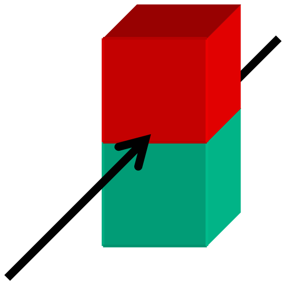

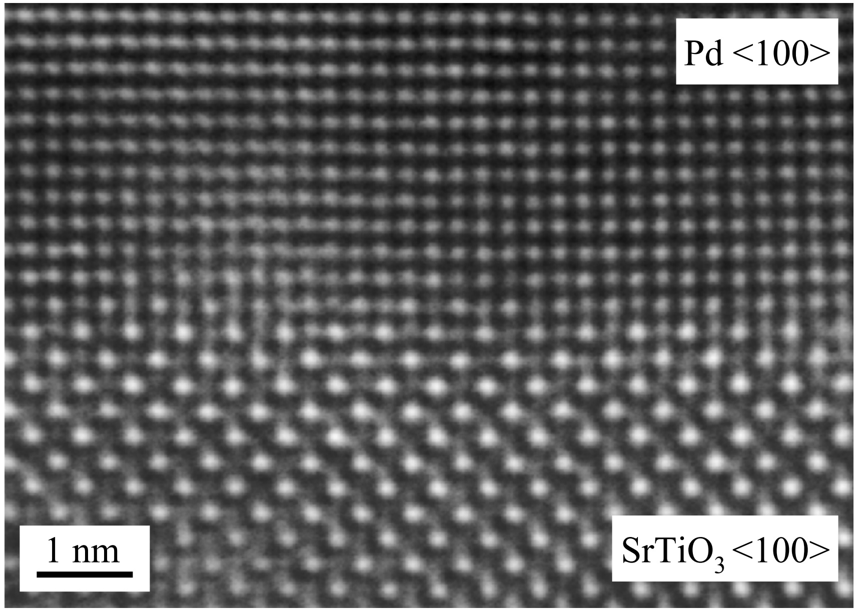

JEM-2010F (Ljubljana)

<110>

Viewing direction

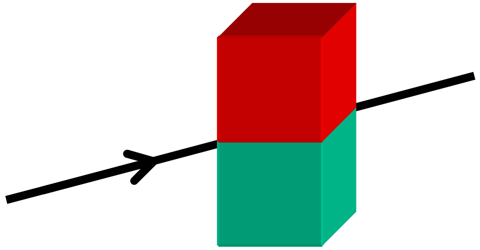

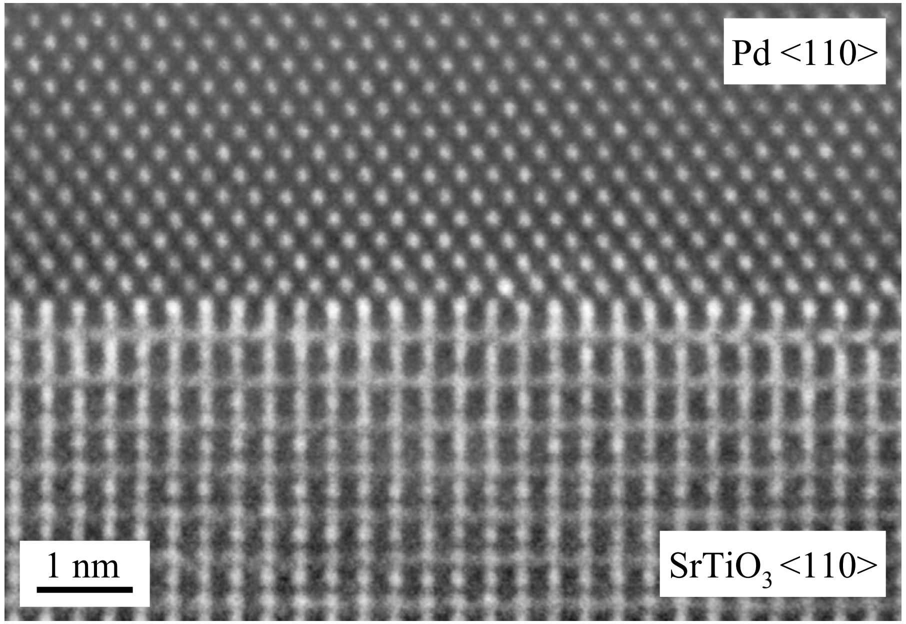

JEM-ARM 1250 (Stuttgart)

Quantitative HRTEM Analysis of Pd/$SrTiO_3$

- High quality HRTEM images of Pd/$SrTiO_3$ interface have been obtained

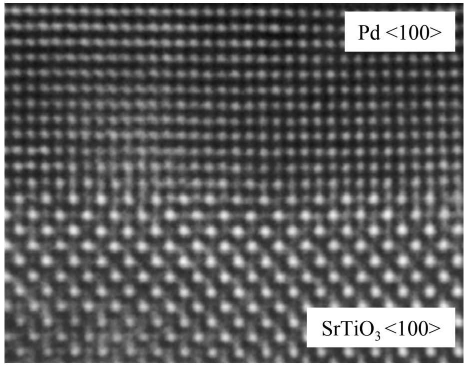

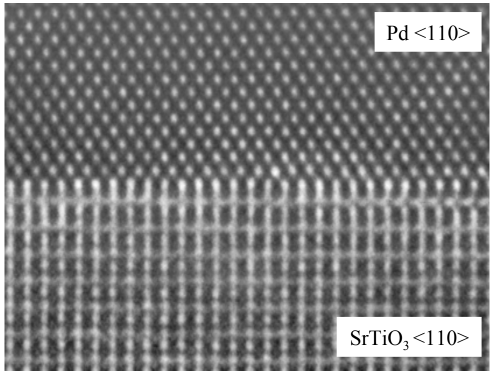

- Projected bonding distance of 2.133 Å (QHRTEM) between Pd and $SrTiO_3$

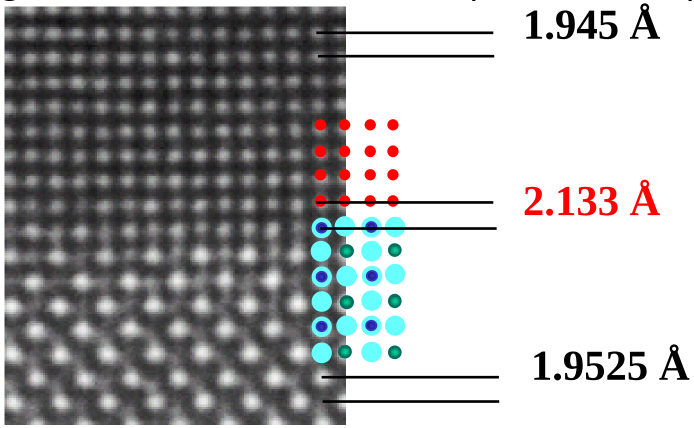

- $SrTiO_3$ is terminated by TiO_2 layer
- Pd atoms sit on top of O ions
- No distortion of Pd or $SrTiO_3$ adjacent to interface could be determined

Theoretical Studies: *Ab-initio* Calculations

TiO_2 Termination

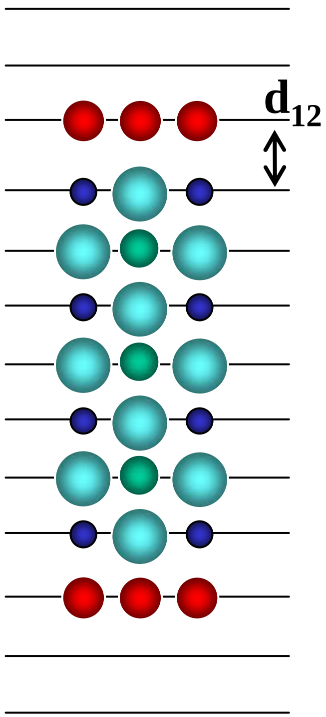

Atom positions

1 Pd ML	d_{12}, Å	s, Å
Pd/O	2.14	-0.05
Pd/Ti	2.43	-0.05

2 Pd ML		
Pd/O	2.15	-0.05
Pd/Ti	2.53	-0.05

3 Pd ML		
Pd/O	2.16	-0.06
Pd/Ti	2.48	-0.05

Cohesion Energy, eV

Pd ML	Pd/O	Pd/Ti
1	-2.97	2.84
2	-3.57	-3.44

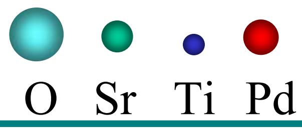

SrO Termination

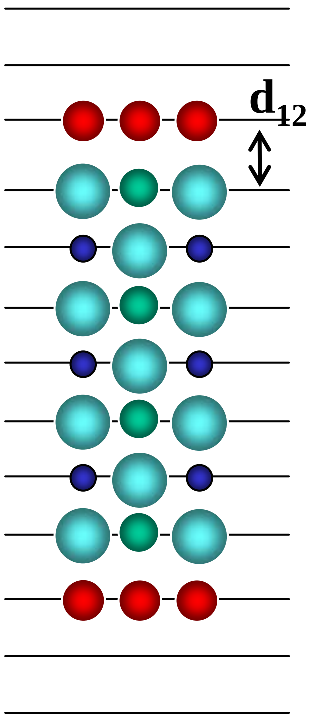

Atom positions

1 Pd ML	Pd-O Å	Pd-Sr Å	s, Å
Pd/O,Sr	2.07	2.83	0.17
Pd/□	2.92	3.09	0.23

2 Pd ML			
Pd/O,Sr	2.16	2.76	0.22
Pd/□	3.00	3.18	0.22

Cohesion Energy, eV

Pd ML	Pd/O,Sr	Pd/□
1	-2.90	-2.58
2	-3.54	-3.44

- TiO_2 termination is energetically favoured
- Pd prefer to position on top of the O atoms
- The projected bonding distance at the interface differ from both bulk parameters (increased)

ELNES Spectra by Spatial Difference Technique

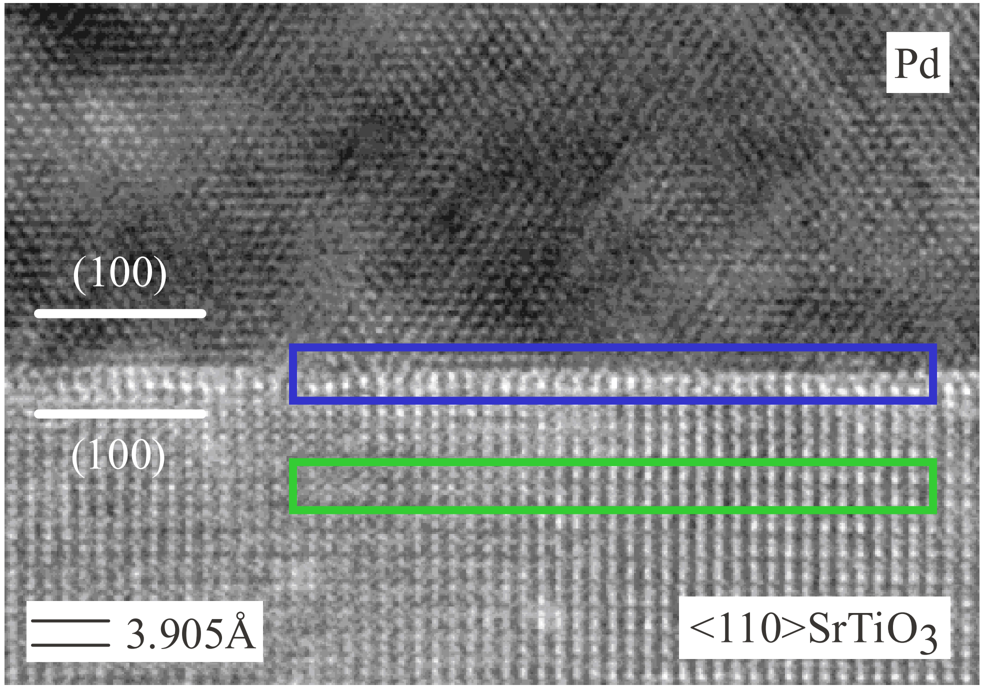

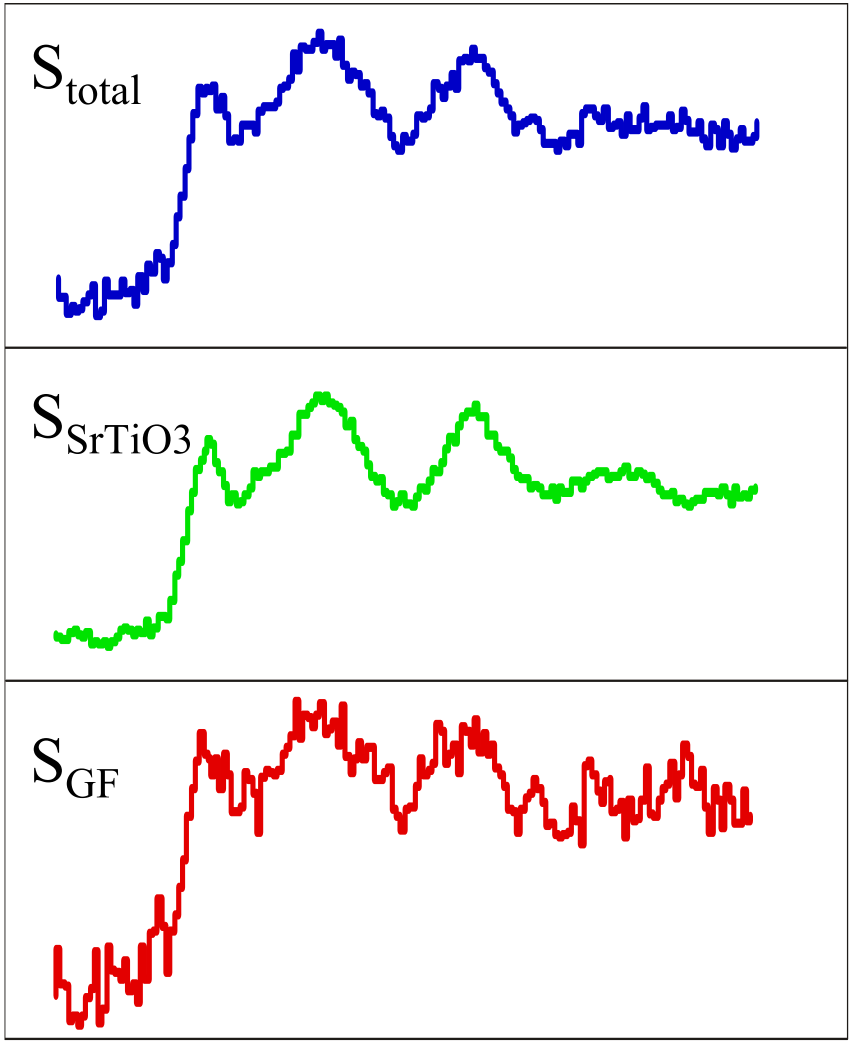

fine structure of O-K edge

- interface specific ELNES component S_{GF}:

$$S_{GF} = S_{total} - \mu\, S_{SrTiO_3}$$

- scaling factor μ: geometric considerations

K. van Benthem (2003)

Termination of the Substrate Surface

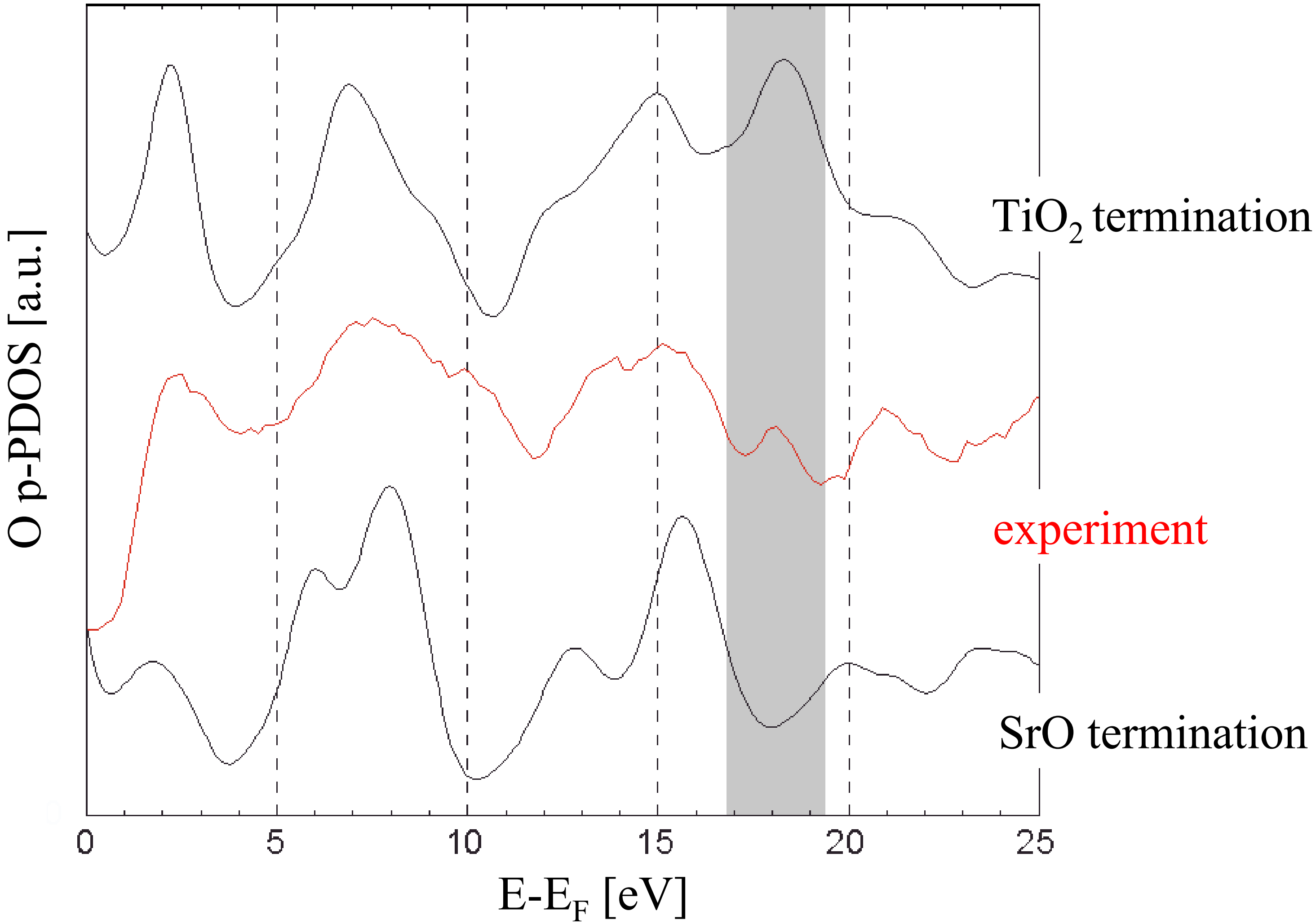

The Pd/$SrTiO_3$ interface
- *Ab-initio* calculations -

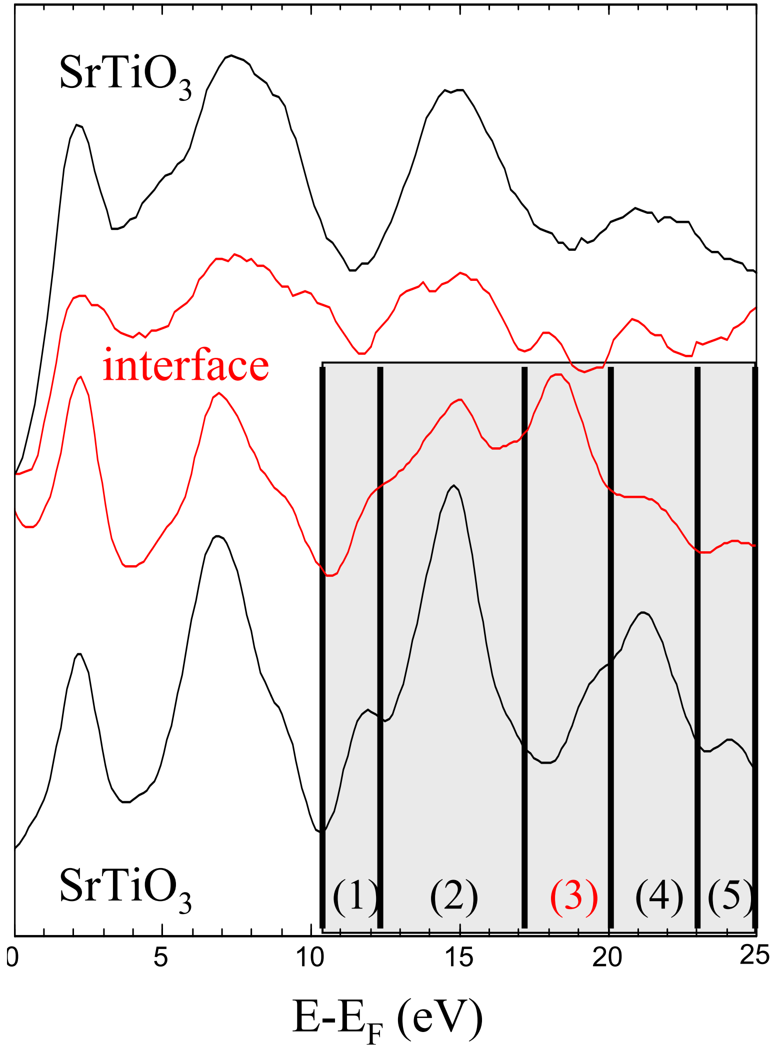

ELNES Structure

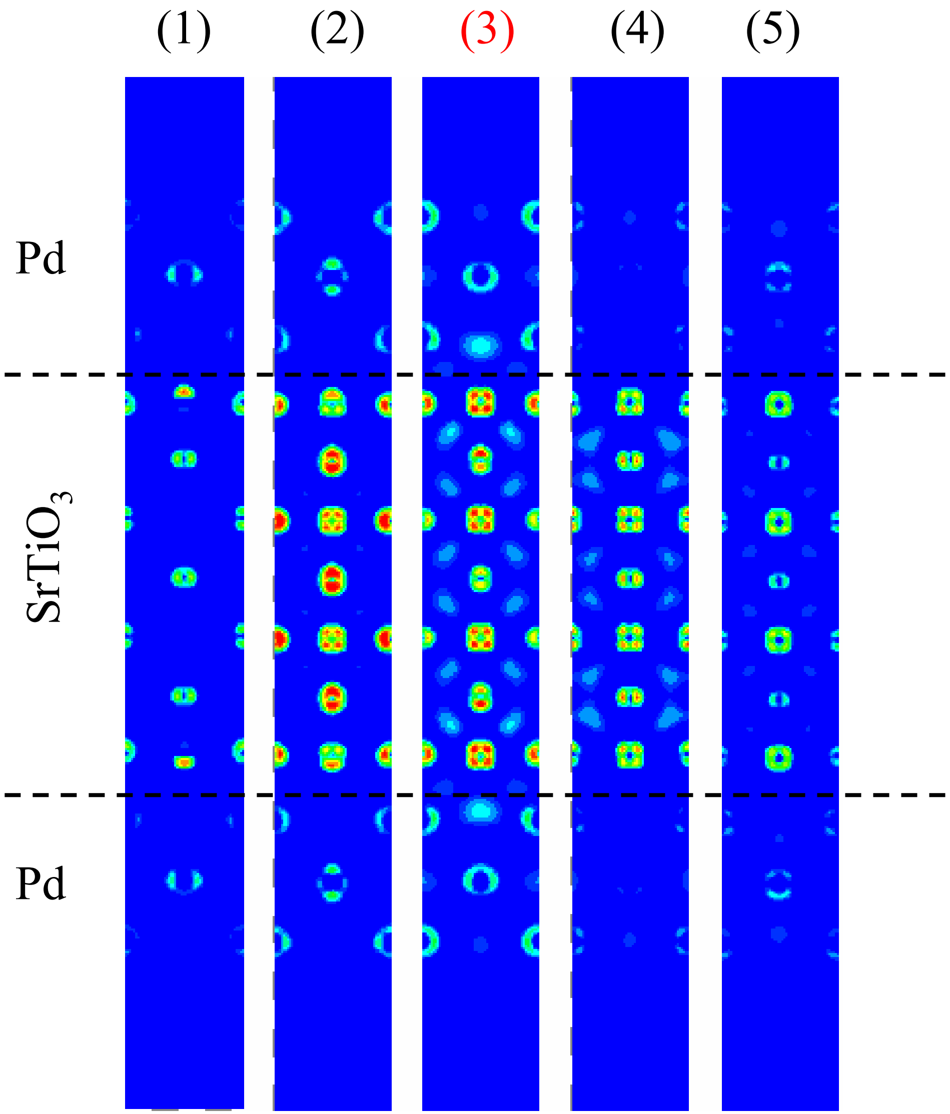

Summary and Conclusions

Advances TEM Techniques allow the characterisation of defects to the atomic level

- Q-HRTEM $\Rightarrow$ Structure
- Q-AEM $\Rightarrow$ Composition
- Q-HRTEM $\Rightarrow$ Bonding

Information can be obtained with high precision for special boundaries and interfaces

Correlation to specific properties for STO: Conductivity and diffusivity

Challenge: General Boundary